AMMRC 76-3

NOISE ABATEMENT AND INTERNAL VIBRATIONAL ABSORPTION IN POTENTIAL STRUCTURAL MATERIALS

March 1976

L. Kaufman, S. A. Kulin, P. P. Neshe

ManLabs, Inc.
21 Erie Street
Cambridge, Massachusetts 02139

Semi-Annual Report Contract Number DAAG46-74-C-0048

Sponsored by: Defense Advanced Research Projects Agency
ARPA Order No. 2555

Program Code No. A13719
Effective Date of Contract: 30 November 1973
Contract Expiration Date: 30 December 1976
Amount of Contract: $615,322.00
Contract Period Covered by Report: 1 March 1975 to
1 September 1975

Prepared for

ARMY MATERIALS AND MECHANICS RESEARCH CENTER
Watertown, Massachusetts 02172

UNCLASSIFIED

SECURITY CLASSIFICATION OF THIS PAGE (When Data Entered)

REPORT DOCUMENTATION PAGE		READ INSTRUCTIONS BEFORE COMPLETING FORM
1. REPORT NUMBER AMMRC CTR 76-3	2. GOVT ACCESSION NO.	3. RECIPIENT'S CATALOG NUMBER
4. TITLE (and Subtitle) NOISE ABATEMENT AND INTERNAL VIBRATIONAL ABSORPTION IN POTENTIAL STRUCTURAL MATERIALS		5. TYPE OF REPORT & PERIOD COVERED Semi-Annual Report #3 1 March 1975-Sept. 1 1975
		6. PERFORMING ORG. REPORT NUMBER
7. AUTHOR(s) L. Kaufman S. A. Kulin P. P. Neshe		8. CONTRACT OR GRANT NUMBER(s) DAAG46-74-C-0048
9. PERFORMING ORGANIZATION NAME AND ADDRESS		10. PROGRAM ELEMENT, PROJECT, TASK AREA & WORK UNIT NUMBERS D/A Project: AMCMS Code: Agency Accession:
11. CONTROLLING OFFICE NAME AND ADDRESS Army Materials and Mechanics Research Center Watertown, Massachusetts 02172		12. REPORT DATE January, 1976
		13. NUMBER OF PAGES 56
14. MONITORING AGENCY NAME & ADDRESS(if different from Controlling Office)		15. SECURITY CLASS. (of this report) Unclassified
		15a. DECLASSIFICATION/DOWNGRADING SCHEDULE

16. DISTRIBUTION STATEMENT (of this Report)

Approved for public release; distribution unlimited.

17. DISTRIBUTION STATEMENT (of the abstract entered in Block 20, if different from Report)

18. SUPPLEMENTARY NOTES

ARPA Order: 2555
AMCMS Code: 690000.21. 10846
Agency Accession: DA OE 4778

19. KEY WORDS (Continue on reverse side if necessary and identify by block number)

Titanium-nickel alloys
Vibration damping
Sound transmission
Internal friction
Iron-Cobalt Alloys
Copper-Aluminum-Nickel Alloys

20. ABSTRACT (Continue on reverse side if necessary and identify by block number)

Efforts have been directed toward achieving higher yield strengths in high damping cobalt-iron base alloys by adding nickel, aluminum and manganese. Substantial increases have been achieved through aluminum and manganese additions at low levels. The range of loss factors and yield strengths which are attainable exceed currently available commercial materials. Measurement of the temperature dependence of the loss factor of the cobolt-iron alloy for comparison with Nitinol and

DD FORM 1 JAN 73 1473 EDITION OF 1 NOV 65 IS OBSOLETE

UNCLASSIFIED

SECURITY CLASSIFICATION OF THIS PAGE (When Data Entered)

Incramute show that the cobalt-iron alloy retains a high loss factor up to 120°C while the latter materials exhibit a drop in loss factor well below 100°C.

The effects of alloying additions of iron and manganese as well as reduction in grain size are being investigated as a means for reducing the brittleness of copper-aluminum-nickel alloys which exhibit thermoelastic martensitic transformations. These transformations provide high damping characteristics and high loss factors.

FOREWORD

This research was supported by the Advanced Research Projects Agency of the Department of Defense and was monitored by the Army Materials and Mechanics Research Center under Contract No. DAAG46-74-C-0048.

TABLE OF CONTENTS

LIST OF TABLES

LIST OF FIGURES

LIST OF FIGURES (continued)

Page

I. INTRODUCTION AND SUMMARY

The utilization of structural materials capable of suppressing noise and vibration offers substantial advantages in the design of a wide range of military applications. In particular ship and helicopter propulsion, tracked land vehicle and torpedo propulsion systems would all operate more efficiently if materials capable of absorbing noise and vibration were available for incorporation into the structure.

The present study is aimed at identifying potential structural materials which exhibit high damping capacity (or loss factors) at frequencies in the audible range (i.e. 20-4000 cycles per second) and evaluating the mechanism by which damping takes place. In addition characterization of the mechanical properties such as yield strength and Youngs modulus has also been carried out to evaluate the potential use of the material as a structural element. Finally cost and fabrication factors have also been considered in order to gain some insight into the practical application of these materials in specific military systems.

Novel damping materials such as Nitinol (Ni-Ti) and copper-aluminum-nickel alloys which appear to derive their damping characteristics from thermoelastic martensitic transformations have been investigated. The results have been documented in previous reports (1,2).* In addition, commercial damping materials such as Nivco (Co-Ni-Ti-Al) and Incramute (Cu-Mn-Al) have also been evaluated in order to develop a basis for comparison. In the course of the present study (2) a family of cobalt-iron alloys which can be carefully heat treated to yield very high damping characteristics has been synthesized. Although the mechanism leading to the high loss factors which characterize these alloys is not clear, it appears that the structure which provides the desirable high loss factor is a metastable fcc solid solution. The

---

*Underscored numbers in parentheses denote references.

80 w/o Co-20 w/o Fe alloy, which is the base for this family, is readily cast, forged and cold worked, has been fabricated into rod by swaging and cold rolled into 50 mil foil so that it could be employed in a variety of applications.

Figure 1 shows a bar graph comparing the loss factors of a number of materials under investigation at present in our study. The 0.2 percent offset yield strength is also shown for each material (please note that the loss factor is shown on logarithmic scale). The commercial materials Nivco and Incramute are in the condition supplied by commercial vendors. The results for Nitinol displayed in Figure 1 have been optimized (2) by applying a 15% reduction in thickness by rolling at room temperature. The bar graphs for Co-Fe, Co-Fe-Al and Co-Fe-Mn represent data taken on annealed samples of the experimental alloys currently under study which have been synthesized in the present program. All of the data displayed in Figure 1 refer to 25°C. The loss factors reported were determined by the resonant dwell method (1,2) using a cantilevered beam at a peak stress of 2000 psi. It is well known that many materials show increased loss factors at higher stress (3-8). Indeed such performance may be of critical importance in actual design. Similarly loss factors (Q^{-1}) are known to vary substantially with frequency and usually increase as the frequency is decreased from the audible range to the 1 cycle/sec range. However present consideration has been restricted to frequencies near 200 Hertz (cycles/sec) at low stress levels.

Figure 1 shows that the Co-Fe alloy can develop loss factors near 0.04 (i.e. 4 percent). However the yield strength is low, 18000 psi. The closest competitor is Incramute which exhibits a loss factor of 2 percent. However Incramute has a higher yield strength, 45000 psi. The remaining commercial material, Nivco, has a low damping capacity near 0.1 percent but a high yield strength of 108,000 psi.

During the past six months efforts have been directed

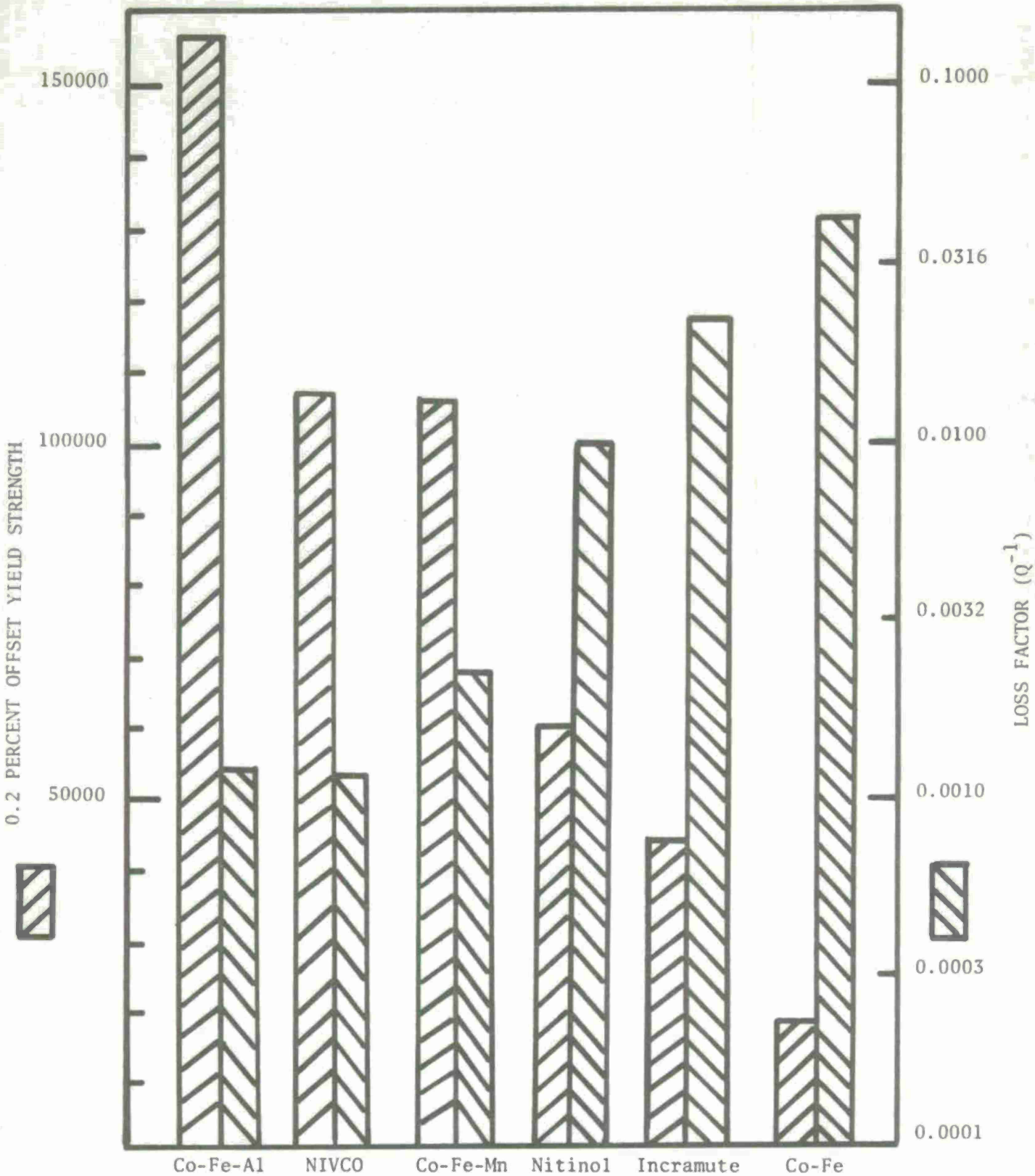

Figure 1. Comparison of Loss Factors and Yield Strength at 25°C for Several Materials. Loss Factor is measured at 2000 psi peak stress and 150-250 Hertz.

towards achieving higher yield strengths in the Co-Fe alloy by additions of nickel, aluminum and manganese. The bar graph in Figure 1 shows results obtained with small additions of aluminum and manganese. In the former case very high yield strengths in excess of 150,000 psi were attained. However this alloy exhibited a loss factor of only 0.1 percent (i.e. like Nivco). Addition of manganese resulted in yield strengths over 100,000 psi coupled with loss factors near 0.3 percent. Thus it appears that a range of loss factors and yield strengths are attainable via alloying the Co-Fe base composition. Current efforts are directed toward optimization of these properties.

An additional facet of the damping factor/mechanical property characteristics of these materials is shown in Figure 2 where the temperature dependence of the loss factor is shown for Nitinol, Incramute and the cobalt-iron alloys. These results indicate that the cobalt-iron alloy maintains high damping characteristics up to 110°C. By contrast Incramute and Nitinol display loss factors below 0.4 percent (i.e. one-tenth that of Co-Fe) above 80°C. Clearly the cobalt-iron alloy offers considerable advantages as a damping material.

During an earlier phase of the present study, high damping behavior was encountered in single crystals of a Cu-Al-Ni alloy (2). Since practical application of this material would require utilization of polycrystalline material, investigation of the effects of grain size on the thermoelastic martensitic transformation temperatures has been initiated. In addition, the effects of grain size and further alloying additions of iron and manganese are being undertaken to reduce the brittleness of this alloy.

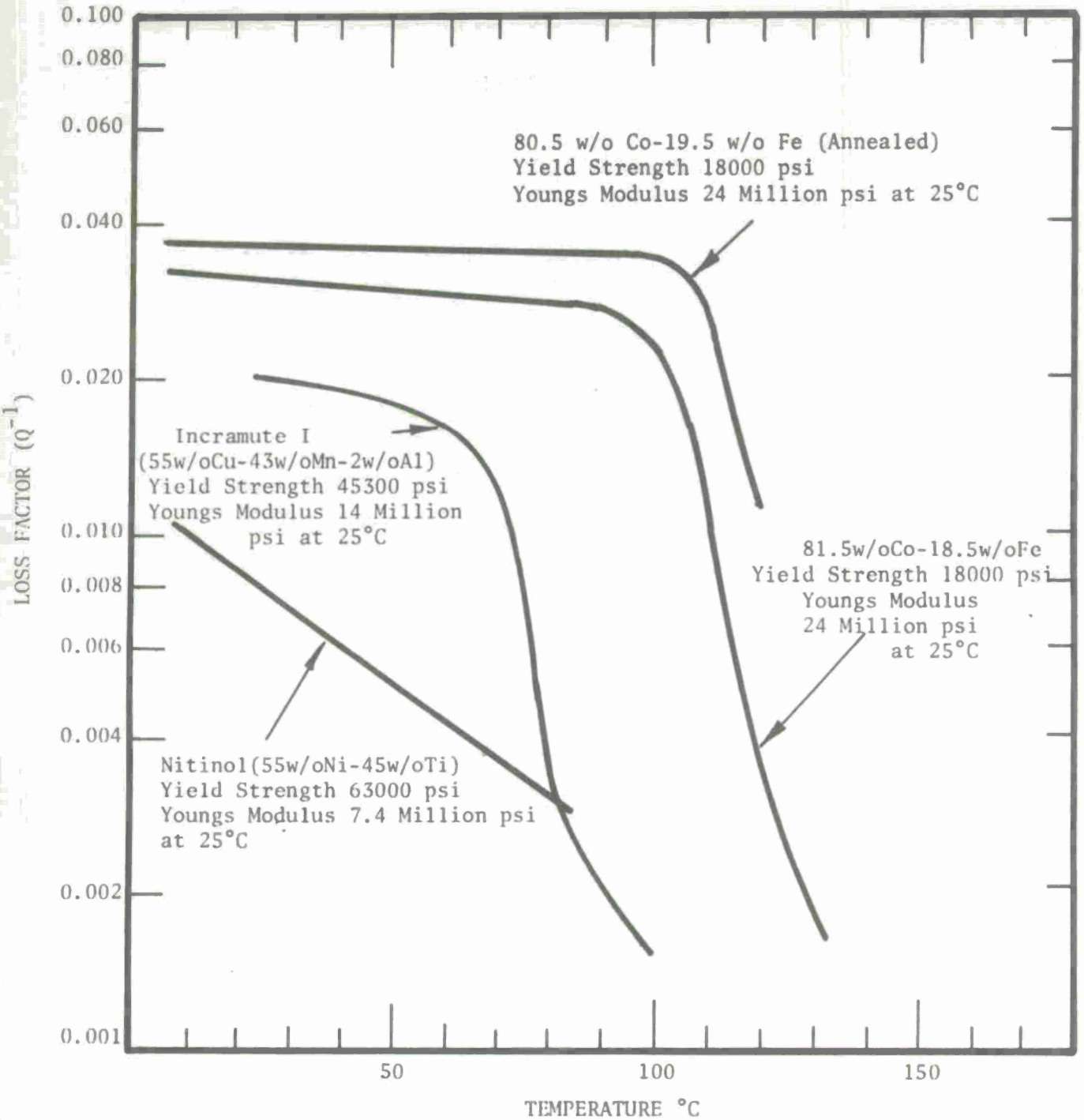

Figure 2. Comparison of the Loss Factor-Temperature Curves for Nitinol, Incramute I and Cobalt-Iron Alloys measured at a stress of 2000 psi in the Frequency Range from 150 to 250 Hertz.

II. INVESTIGATION OF COBALT-IRON ALLOYS FOR APPLICATION AS HIGH DAMPING STRUCTURAL MATERIALS

Current efforts which have been directed toward exploiting the properties of cobalt-iron alloys for the purposes of achieving high damping properties coincident with high strength (2) stem from the work of Cochardt (3,4) who reported on loss factors of 70 w/o Co-30 w/o Ni and Co-Fe alloys at room temperature as disclosed by torsional pendulum measurements at a frequency of one cycle/sec (i.e. one Hertz). Cochardt reported a logarithmic decrement at 25°C and a stress of 2000 psi for a 65 w/o Co-35 w/o Ni alloy of 0.18. The logarithmic decrement is the product of π times Q^{-1}. Thus

$$\zeta = \pi Q^{-1} \tag{1}$$

and if ζ=0.18 then $Q^{-1} \approx 0.06$. This value is approximately fifteen times larger than the value measured in our studies (2). However, the latter values were observed at 200 Hertz (200 cycles/sec) and 2000 psi rather than 1 cycle/sec and 2000 psi stress (2). Cochardt also reported on a 80 w/o Co-20 w/o Fe alloy which exhibited ζ=0.09 (i.e. Q^{-1}=0.03) at 1 cycle/sec and 2000 psi and 25°C. This alloy also exhibits a high Curie temperature. However, in the condition as fabricated by Cochardt (3), this alloy was a stable bcc structure which was probably ordered with no chance for transformation. The processing sequence followed by Cochardt called for homogenization at 1100°C for two hours. Figure 3 shows that the alloy was in the fcc field at this temperature (1373°K). Subsequently the alloy was annealed for two hours at 900°C (1173°K). Figure 3 shows that at this temperature the alloy was still in the stable fcc field but just about to enter the two phase fcc+bcc field. The final step in the processing sequence employed by Cochardt was a slow cool to room temperature at the rate of 120°C/hour. During this treatment the sample enters the region where the bcc

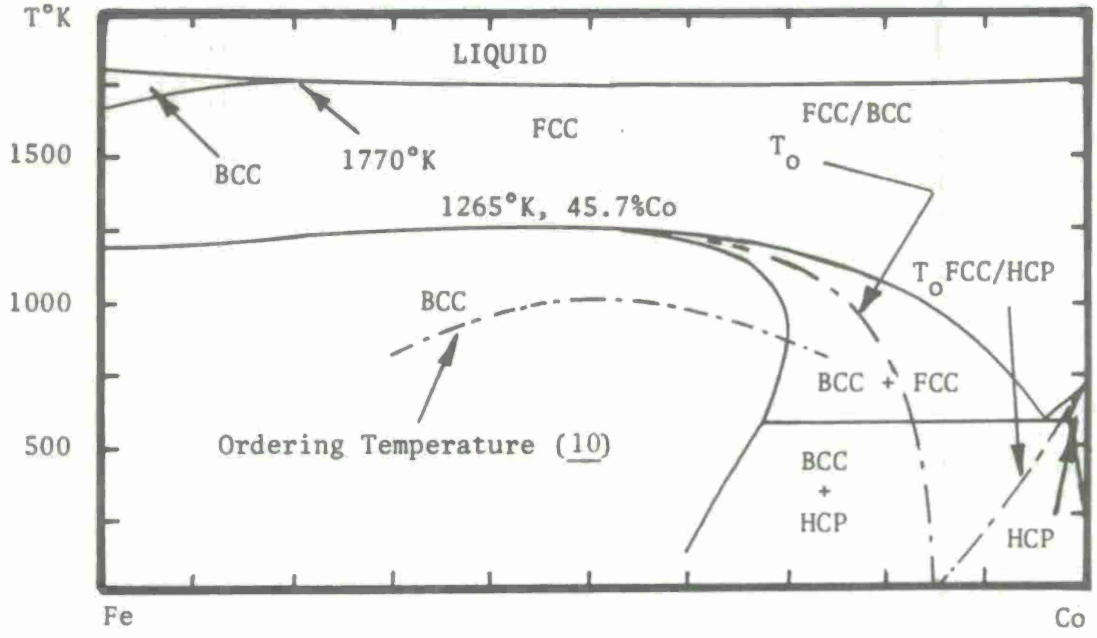

Figure 3. Calculated Iron-Cobalt Phase Diagram Showing Locus of Curve for T_o(FCC/BCC) where FCC and BCC Phases of Same Composition Have Equal Free Energies (9,10).

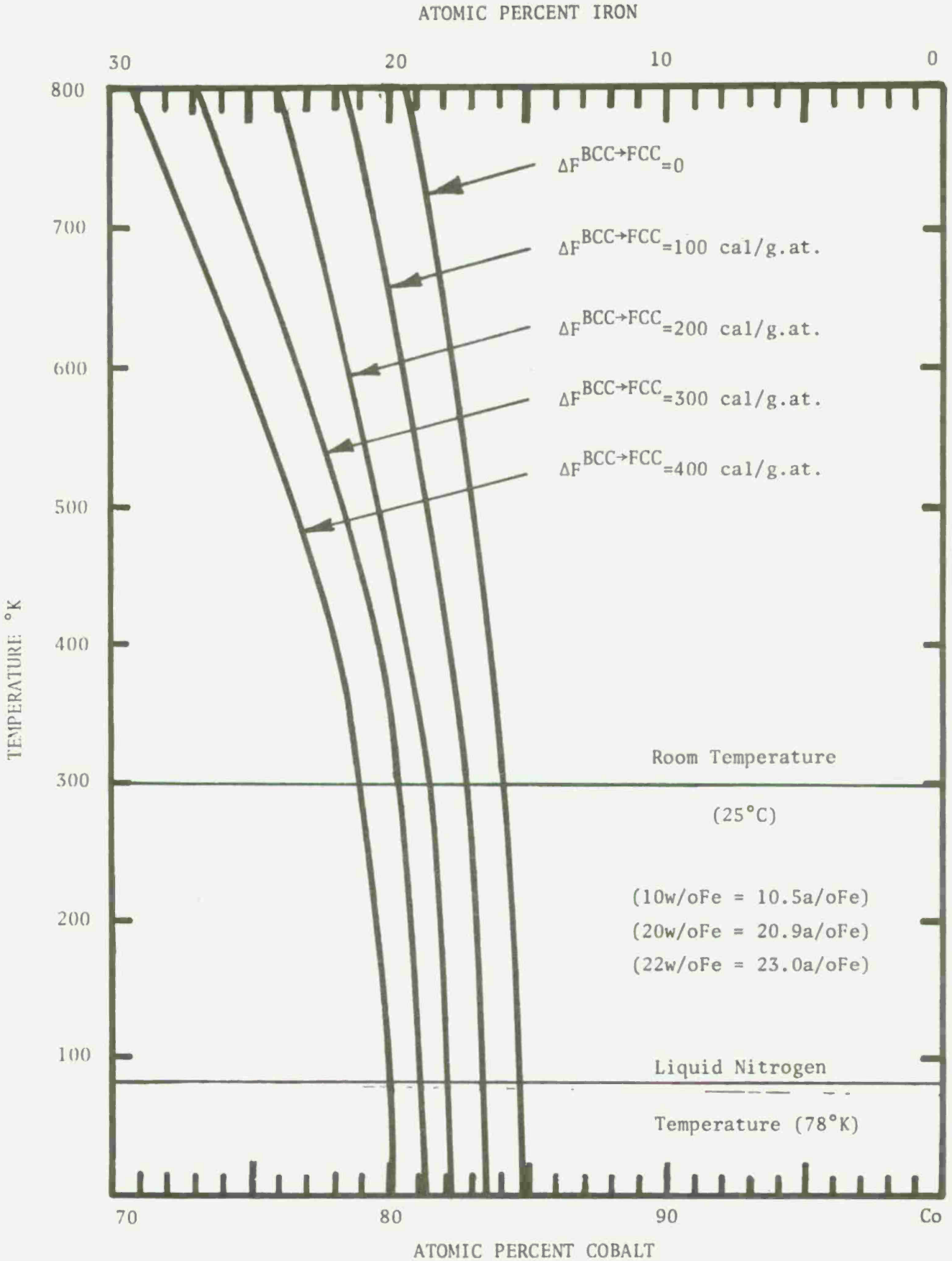

Figure 4. Calculated Temperature and Composition of the Free Energy Difference between FCC and BCC Iron Cobalt Alloys.

phase is stable and coexists with a fcc phase enriched in cobalt. In addition, the bcc orders below 800°K as is seen in Figure 3. Unfortunately Cochardt did not discuss the structure of his 80Co-20Fe alloy. However, based on his heat treatment schedule, it is likely that his alloy was largely bcc.

Figure 3 shows a curve labeled $T_o^{FCC/BCC}$ which describes the locus of points along which the fcc and bcc Co-Fe alloys have equal free energies. This curve has been computed using a thermochemical description of the fcc and bcc phases derived earlier. Figure 4 shows the free energy difference between the fcc and disordered bcc phases as a function of temperature and composition. The curve labeled $\Delta F^{BCC \rightarrow FCC}=0$ is the same as that shown in Figure 3. The remaining curves show the locus of points corresponding to various free energy differences between disordered fcc and bcc phases. As the free energy difference becomes larger, the bcc becomes more stable relative to the fcc phase for a given composition. In the case of iron base alloys (i.e. Fe-Ni and Fe-C alloys), the fcc phase can be retained by rapid cooling until the "driving force" for transformation to the bcc form reaches the vicinity of 300 cal/g.at. (i.e. the free energy of the bcc phase is 300 cal/g.at. less than the fcc phase). Figure 4 suggests that this situation should prevail at room temperature in an alloy with 80 a/o Co-20 a/o Fe (80.9 w/o Co-19.1 w/o Fe). Alloys containing less than 20 a/o Fe could be expected to remain fcc while alloys with greater than 20 a/o (19.1 w/o) Fe would be expected to transform to the bcc phase on cooling from 1000°C. In order to test this prediction, a series of cobalt-iron alloys was prepared and air cooled from 1000°C. Figures 5-8 show the resulting microstructures. The first two photomicrographs show typical austenitic fcc structures obtained by air cooling the 82 w/o Co-18 w/o Fe and 90 w/o Co-10 w/o Fe alloys. On the other hand, Figure 57 shows the martensitic bcc structure obtained on air cooling the 78 w/o Co-22 w/o Fe alloy. The crystal structure

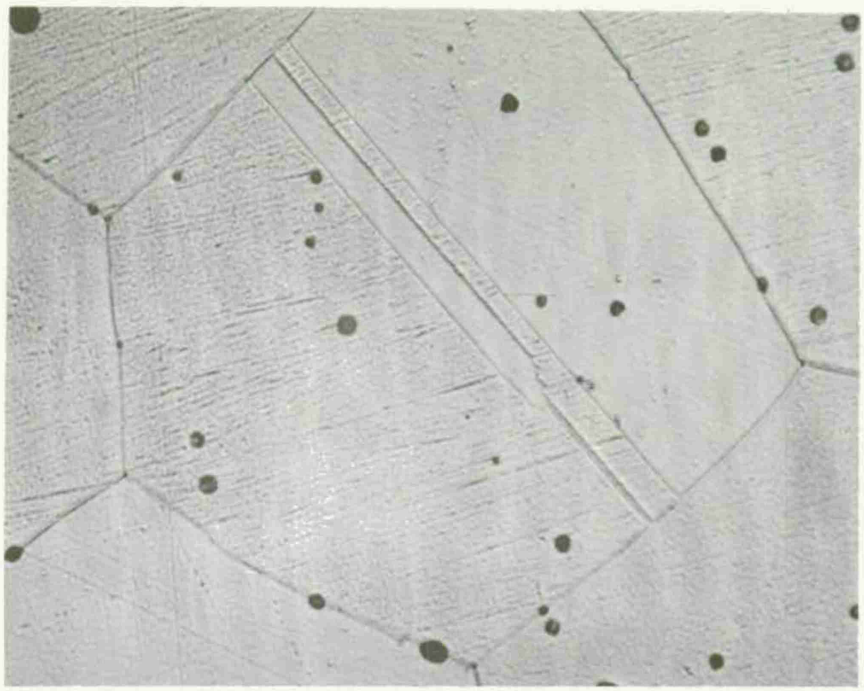

Plate No.
10486

Figure 5. 82 w/o Co-18 w/o Fe Alloy Annealed at 1000°C Air Cooled to 25°C. Etched in 5% Nital. Photomicrograph Shows Twinned Austenitic Structure (X1000).

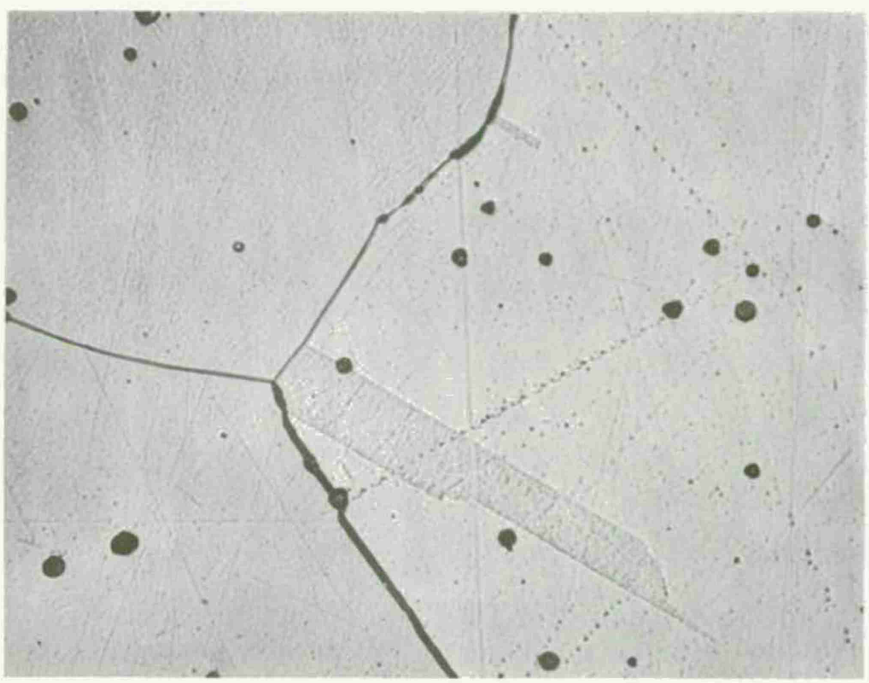

Plate No.
10489

Figure 6. 90 w/o Co-10 w/o Fe Alloy Annealed at 1000°C Air Cooled to 25°C. Etched in 5% Nital. Photomicrograph Shows Twinned Austenitic Structure (X1000).

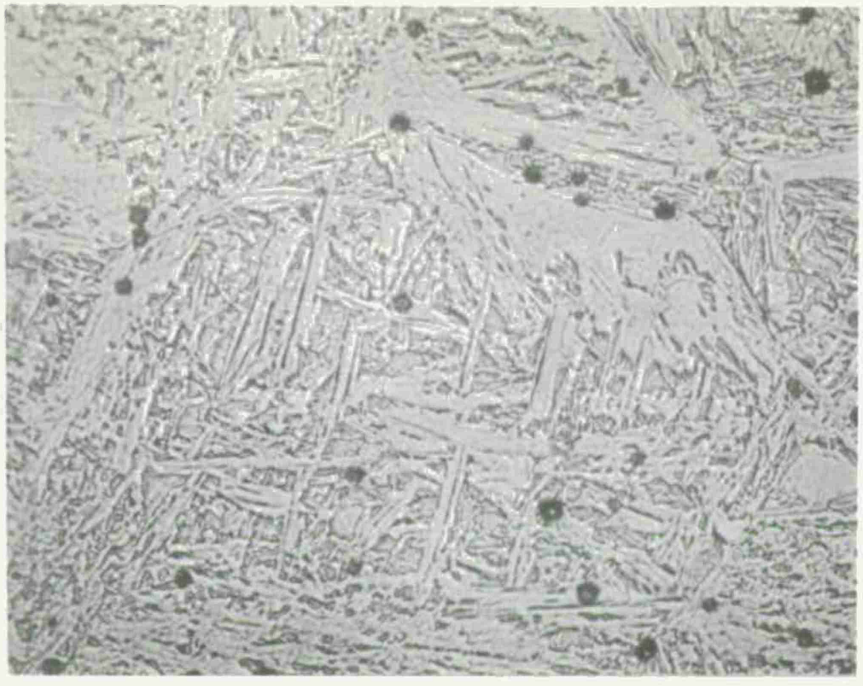

Plate No.
10483

Figure 7. 78 w/o Co-22 w/o Fe Alloy Annealed at 1000°C Air Cooled to 25°C. Etched in 5% Nital. Photomicrograph Shows Structure of BCC Phase (X1000).

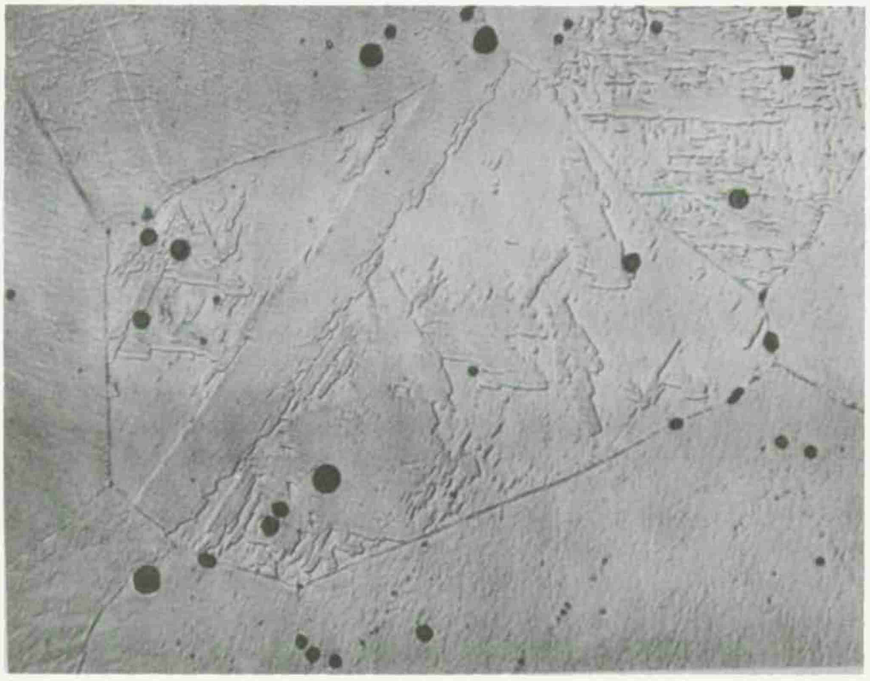

Plate No.
10484

Figure 8. 80 w/o Co-20 w/o Fe Alloy Annealed at 1000°C Air Cooled to 25°C. Etched in 5% Nital. Central Grain Shows Surface Martensite (BCC) Formed during Polishing in an Austenite (FCC) Matrix (X1000).

of these alloys was verified by x-ray diffraction using CrKα radiation. Inclusions shown in Figures 5-8 are oxide particles which are present in the Ferrovac E iron used to make the alloy by combination with electrolytic cobalt.

Figure 8 shows the microstructure of the 80 w/o Co-20 w/o Fe alloy which contained some surface martensite formed during the polishing. This was established by annealing the specimen at 1000°C, air cooling it and taking an x-ray pattern from the surface without polishing. This pattern showned no bcc diffraction lines. However, polishing the surface produced strong bcc peaks. This result suggests that the 20 w/o Fe alloy (19.1 a/o Fe) is close to transforming at room temperature. This result is in keeping with the predictions of Figure 4.

An attempt was made to produce martensite in this alloy by cooling it in liquid nitrogen (i.e. to 77°K). However, no bcc phase formed. This may be due to the steep free energy difference versus temperature curve which does not yield very many more cal/g.at. of driving force as the temperature is lowered from 300°K to 77°K.

The results shown in Figures 5-8 are in keeping with earlier studies of the Co-Fe system (11-13) which showed a lowering of the fcc/hcp transition temperature of cobalt by the addition of iron. Addition of 5 a/o Fe to cobalt reduced T_o from 735°K to 500°K (12,13). Alloys with 7.5, 10.0, 12.5 and 15 a/o Fe cooled to 25°C (248°K) by water quenching after two hours at 1100°C were found to be completely fcc (11). Plastic deformation in Liquid nitrogen by hammering to effect a 17% deformation produced hexagonal phase in the 7.5 a/o Fe alloy and some bcc phase in the 15 a/o alloy. However the 10.0 and 12.5 a/o Fe alloys were found to remain fcc.

Thus, the series of Co-Fe alloys shown in Figures 5 and 8 with 18 and 20 w/o iron fall in exactly the range required to test the hypothesis, i.e. that high damping could be attained in

a metastable phase with a high magnetic Curie point. The Curie point for the fcc appears to be near 950°C (1223°K)(13).

Accordingly, a series of "resonant dwell damping" bars were fabricated from alloys in this series and tested at 25°C along with an additional set of alloys at a stress level near 2000 psi. The geometry of the samples resulted in natural frequencies in the 190-270 Hertz range. The results for the original set of samples are shown in Table 1 (2). This group of samples labeled 51-64 were prepared by annealing alloy stock, machining the damping bars and then making the measurements.

Subsequently, the damping bars were x-rayed. It was found that samples 57, 58, 59 and 60 (i.e. 80 w/o Co-20 w/o Fe and 82 w/o Co-18 w/o Fe) exhibited fcc and bcc diffraction lines. This was apparently due to the surface deformation which occurred during machining. Consequently, these four samples were reannealed at 1000°C and oil quenched. These samples yielded completely fcc x-ray patterns. Subsequent measurement of the loss factor yielded values of 280 to 500 x 10^{-4} as shown by samples 57A, 58A, 59A and 60A in Table 1. Following this experience, the remainder of samples 51-64 were reannealed and oil quenched and the loss factor at 25°C measured once again. The results are shown in Table 2. The reannealing did not affect the loss factors of the 78 w/o Co-22 w/o Fe samples very much. These were 14 and 16 x 10^{-4} (Numbers 55 and 56) before the reannealing and 20 and 13 x 10^{-4} (Numbers 55A and 56A) after reannealing. The diffraction patterns both showed substantial quantities of the bcc phase. Similarly, the reannealing had little effect on the 90 w/o Co-10 w/o Fe alloys. The samples 61 and 62 exhibited Q^{-1}=8 and 14 x 10^{-4} before reannealing and 7 and 7 x 10^{-4} after annealing. Both sets of x-ray patterns showed completely fcc structures. Thus the results show a marked peak in the loss factor in the vicinity of 80 w/o Co-20 w/o Fe providing the alloy is all fcc. This is not dependent on the magnetic Curie temperature since both the fcc and bcc phases have high Curie temperatures which

TABLE 1

SUMMARY OF RESONANT DWELL DAMPING MEASUREMENTS AT 25°C

Sample No. Composition (weight percent)	Resonant Frequency (Hz.)	Dynamical Youngs Modulus ($PSIx10^{-6}$)	Peak Stress (PSI)	Loss Factor ($Q^{-1}x10^{4}$)	Comments on Test
51(70Co-30Ni)	265	28.0	2190	66	All Samples
52(47.2Fe-52.8Pt)	185	15.7	1290	28	Annealed at
53(47.2Fe-52.8Pt)	214	19.2	1660	25	1000°C--Air
54(46.2Fe-53.8Pt)	191	14.7	1290	69	Cooled--Then
55(78.0Co-22.0Fe)	259	26.6	2050	14	Machined
56(78.0Co-22.0Fe)	251	26.3	1980	16	"
57(80.0Co-20.0Fe)	237	24.2	1790	92	"
58(80.0Co-20.0Fe)	251	24.3	1900	68	"
59(82.0Co-18.0Fe)	245	23.1	1800	81	"
60(82.0Co-18.0Fe)	237	22.8	1740	64	"
61(90.0Co-10.0Fe)	264	27.8	2140	8	"
62(90.0Co-10.0Fe)	264	28.1	2140	14	"
63(65Co-28Fe-7Ni)	240	23.2	1770	17	"
64(70Fe-20Co-10Cr)	276	29.9	2410	6	"
57A(80.0Co-20.0Fe)	238	24.4	1810	280	All Samples
58A(80.0Co-20.0Fe)	243	25.5	1990	450	Annealed at
59A(82.0Co-18.0Fe)	236	21.4	1670	480	1000°C and
60A(82.0Co-18.0Fe)	242	23.8	1810	500	Oil Quenched

TABLE 2

SUMMARY OF RESONANT DWELL DAMPING MEASUREMENTS AT 25°C

Sample No. Composition (weight percent)	Resonant Frequency (Hz.)	Dynamical Youngs Modulus ($PSI \times 10^{-6}$)	Peak Stress (PSI)	Loss Factor ($Q^{-1} \times 10^{4}$)	Comments on Test
55A(78.0Co-22.0Fe)	253	25.4	1960	20	All Samples
56A(78.0Co-22.0Fe)	252	26.5	2000	13	Annealed at
61A(90.0Co-10.0Fe)	266	28.2	2170	7	1000°C--Then
62A(90.0Co-10.0Fe)	272	29.8	2270	7	Oil Quenched
63A(65Co-28Fe-7Ni)	244	24.0	1830	28	"
72A(79.0Co-21.0Fe)	249	24.3	1900	19	"
73A(79.0Co-21.0Fe)	264	27.8	2140	10	"
75A(80.0Co-20.0Fe)	249	24.3	1900	24	"
76A(80.0Co-20.0Fe)	251	26.3	1980	274	"
77C(81.0Co-19.0Fe)	232	21.2	2000	11	Machined in 33%
78C(80.5Co-19.5Fe)	248	24.3	2000	12	Cold Worked Condition
79 NIVCO	275	28.3	2000	14	As Received from
79 NIVCO	272	28.2	5000	26	Westinghouse
80C(81.5Co-18.5Fe)	245	23.1	2000	12	Machined--Cold Worked
73B(79.0Co-21.0Fe)	263	27.0	2100	9	Annealed--Water Quenched
77A(81.0Co-19.0Fe)	257	24.8	2000	31	Annealed 1000°C--Then
78A(80.5Co-19.5Fe)	248	24.4	2000	320	Oil Quenched
80A(81.5Co-18.5Fe)	247	24.3	2000	110	"

are near 1000°C.

Table 2 shows additional results for other Co-Fe alloys with compositions in the vicinity of 80 w/o Co-20 w/o Fe which were made and tested in order to establish the effects of composition, structure and degree of cold work on the loss factor. These preliminary results show that the high damping behavior can be reproduced in other alloys but it is eliminated by cold work. This work is proceeding in order to establish the processing limits for obtaining high loss factors.

Table 2 also contains the results of damping tests on NIVCO, which is a commercial alloy developed by Cochardt at Westinghouse (4). It was kindly furnished by Dr. Lou Willertz of Westinghouse Research Laboratories. According to Cochardt's description, NIVCO is 72 w/o Co-23 w/o Ni and the balance titanium and aluminum which are added to provide strength by precipitation hardening. Cochardt reports values of the logarithmic decrement of 0.02 and 0.05 at room temperature for this alloy at shear stresses of 2000 psi and 5000 psi (Figure 1 of Reference 4). Since Q^{-1} is equal to the decrement divided by π, Cochardt's results would correspond to loss factors of 0.007 and 0.017 or 70×10^{-4} and 170×10^{-4} respectively at 25°C and stresses of 2000 psi and 5000 psi. These values are much higher than those shown in Table 2. The values measured in the present tests, i.e. 14×10^{-4} at 2000 psi and 26×10^{-4} at 5000 psi, are five times smaller than Cochardt's results. The main difference is that the frequency of the present measurements at 230-270 Hz is in the audible range while that used by Cochardt was near 1 cycle/sec (1 Hertz).

The results (2) shown in Tables 1 and indicate that loss factors of $Q^{-1} = 500 \times 10^{-4}$ are attainable in the 80 w/o Co-20 w/o Fe alloys which are two to three times higher than observed in nitinol (i.e. 55 w/o Ni-45 w/o Ti) and fifty times higher than NIVCO. Preliminary results on the 80 w/o Co-20 w/o Fe alloy show almost no change in the audible "ring" (or lack of

"ring") of the alloy at liquid nitrogen or +200°C. Thus it is not anticipated that the Q^{-1} value will decrease significantly in this temperature range.

The other advantages the Co-Fe alloy has in relation to the Ni-Ti alloy are a higher modulus of 25 million psi (Tables 1 and 2) versus 8 million psi and the ease with which the Co-Fe alloy can be fabricated.

In order to evaluate the strength of the 80 w/o Co-20 w/o Fe composition, a set of tensile bars were fabricated of annealed material. Subsequent tests were expanded to test swaged rod. These were compared with tensile results measured for NIVCO (2). The 82 w/o Co-18 w/o Fe and 80 w/o Co-20 w/o Fe alloys show reproducible 0.2 percent offset yield strengths of 17000-18000 psi in the annealed condition. This is the strength level of the samples which exhibited loss factors of $Q^{-1} = 500 \times 10^{-4}$. The yield strength was also measured for samples of the 18.5 w/o Fe, 19 w/o Fe and 19.5 w/o Fe alloys in a cold worked condition following a 33% reduction in diameter by cold swaging. In this condition yield strengths near 70,000 psi were observed (2). Reference to Table 2 shows that these alloys exhibited loss factors of 11 to 14 $\times 10^{-4}$ in the cold worked condition. Annealing raised the loss factor of the 19.5 w/o Fe sample to 320×10^{-4} as shown in Table 2.

Tensile tests on NIVCO produced a 0.2 percent yield strength of 108,900 psi (2) in good agreement with Cochardt's reported value of 110,000 psi (4).

These values of the yield strength were combined with the measured loss factors measured at a stress level of 2000 psi in the range 150 to 250 Hz for NIVCO, 80 w/o Co-20 w/o Fe and 55 w/o Ni-45 w/o Ti are compared in Figure 1. The comparison shows the relatively high damping capacity (and low strength) of the Co-Fe alloy to the other two materials. However, it is likely that this shortcoming can be overcome through alloying. For example, the strength of NIVCO is not due to the properties

of the 72 w/o Co-23 w/o Ni matrix, which is comparable to the 80 w/o Co-20 w/o Fe material. The strength is due to the presence of precipitates formed by the Al and Ti additions. A similar effect can be expected in the Co-Fe alloy. Another possible source of strengthening is additional solid solution hardening which might be effected by addition of nickel. The nickel additions would be controlled so as to maintain the "metastable condition" of the fcc phase. This is illustrated in Figure 9 which shows the ternary Fe-Ni-Co counterpart of Figure 3 calculated on the basis of the thermochemical description published previously (9).

Figure 9 shows the locus of the $\Delta F^{BCC \rightarrow FCC}=0$ and the $\Delta F^{BCC \rightarrow FCC}=+300$ cal/g.at. curves in the Fe-Ni-Co system at 25°C. These alloys should be metastable in the fcc form at 25°C. If they can be fabricated in this state, they may develop high Q^{-1} values comparable to 80 w/o Co-20 w/o Fe and higher yield strengths than the 17,500 psi level exhibited by the 80/20 Co-Fe alloy. Such a series of alloys is currently being fabricated for evaluation. If this effort produces the desired result, it would also have a beneficial effect on the cost of the alloys since it would increase the iron content of the alloy and substitute nickel for cobalt. Both of these composition changes would lower the cost.

In order to proceed with the development of the 80 w/o Co-20 w/o Fe compositions, two separate routes have been pursued. First, fabrication studies on the base composition have been pursued. Second, alloying studies have been carried out in order to evaluate the effects of additions on the strength and damping capacity. All of the measurement techniques employed in these tests are those which have been detailed in earlier reports (1,2).

Three ten-pound heats of the 80 w/o Co-20 w/o Fe alloy have been vacuum melted and cast into two inch diameter moulds. The ingots were subsequently forged to 3/4 inch bars and then (cold) swaged to 1/2 inch rod. Intermediate anneals of 1000°C

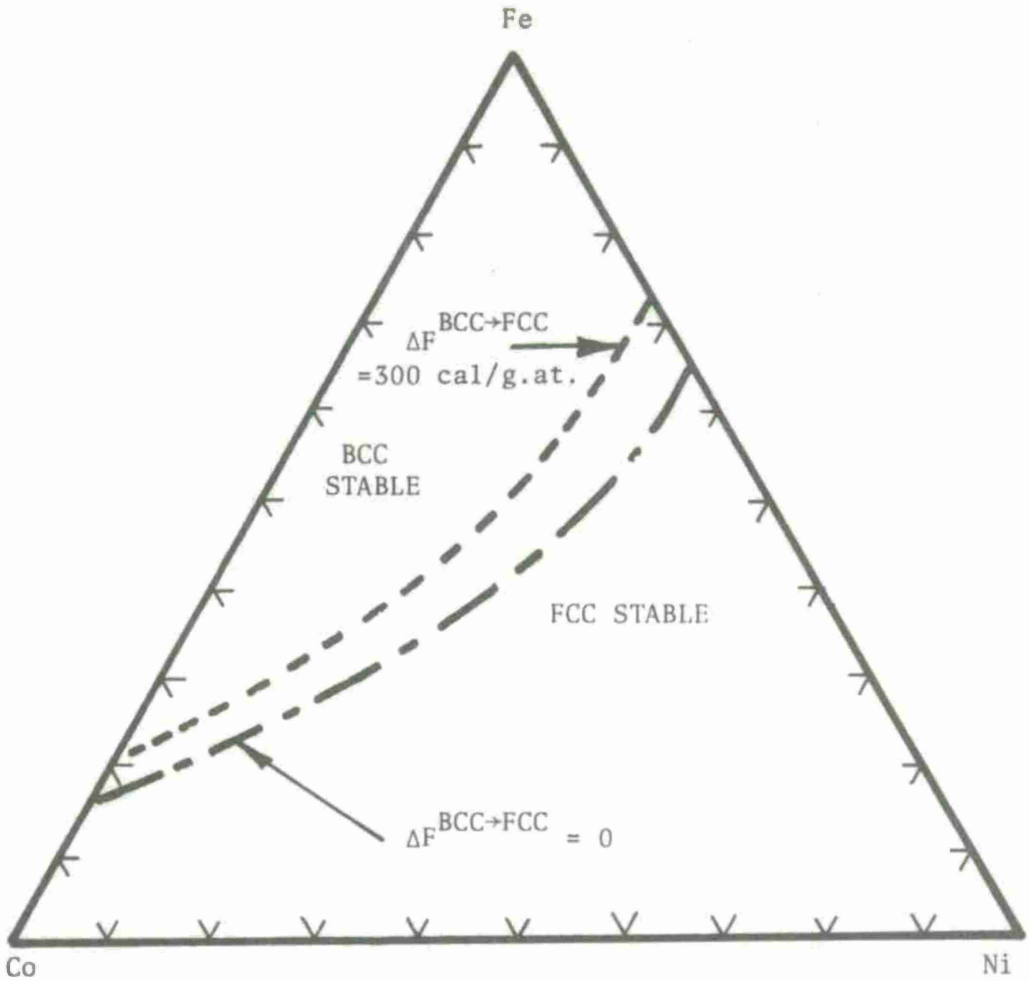

Figure 9 . Calculated Regions of BCC and FCC Stability for Fixed Compositions at 25°C in the Iron-Nickel-Cobalt System.

were employed. The final product was sixty inch long rod. However, it was found that this structure was a mixture of bcc and fcc phases (see earlier discussion) and the rod "rang" when struck, indicating poor damping. However, the high damping characteristics were readily restored by proper heat treatment above 1000°C followed by air cooling. The x-ray analysis of the material disclosed a fully austenitic (fcc) structure and the high damping characteristic of the rod was regenerated.

A second demonstration of the ease with which the 80 w/o Co-20 w/o Fe alloy can be fabricated was the reduction of as-cast 1/2 inch thick slab to 50 mil foil. This was carried out in a series of 20% reductions with intermediate anneals. The reductions were quite moderate and the ease with which they were made indicates that even larger reductions could be successfully carried out. This would certainly appear to be possible if the reductions were carried out by hot rolling. The final treatment of the fifty mil foil consisted of a 1000°C for 30 minutes which yielded soft foil which "rang like lead."

These results indicate that the 80 w/o Co-20 w/o Fe alloy can be readily formed if it is in the fcc condition. Moreover it can be heat treated to yield this structure quite readily. Although it has been established that the two phase (fcc+bcc) structure does not exhibit outstanding damping characteristics, it is probable that rather high strengths could be attained with this structure if it were attained by formation of an ordered bcc phase. This alloy (80 w/o Co-20 w/o Fe) could be readily formed in the fcc structure (as demonstrated above) and then aged to high strength by ordering the bcc phase. In fact, small carbon additions might even be incorporated into such a structure to enhance the strength by conferring some tetragonality into the bcc phase in analogy with ferrous martensites.

Before turning to the alloying studies conducted on the 80 w/o Co-20 w/o Fe alloy it is useful to recount the temperature dependent studies undertaken to establish the data shown in Figure

2. The tests were conducted under the direction of Dr. John Heine of Bolt Beranek and Newman using the techniques detailed earlier (1,2).

Figures 10 and 11 show loss factor versus temperature curves for samples of a 80.5 w/o Co-19.5 w/o Fe and 81.5 w/o Co-18.5 w/o Fe alloy between -60°C and +80°C. Additional samples which were tested between 25°C and 130°C yield the results shown in Figure 2.

In order to obtain an additional set of data on a high damping alloy which is generally available, a sample of Incramute was obtained from Mr. Eugene Thiele of the Copper Development Association Inc. A square plate 5 1/2 inches x 5 1/2 inches x 1/4 inch thick was obtained in the heat treated condition designed to yield maximum damping. This plate was employed to fabricate resonance dwell damping bars (1,2) and tensile bars. Figure 12 shows the results of the damping measurements conducted on the Incramute (55 w/o Co-43 w/o Mn-2 w/o Al) alloy between -60°C and 100°C. Tensile tests conducted at 25°C resulted in a 0.2% offset yield strength of 45,300 psi. These data are shown in Figures 1 and 2.

It is interesting to note that the copper-manganese alloy system, upon which Incramute and several other commercial damping alloys are based was predicted to have a metastable fcc miscibility gap in 1969 (14). Recent experimental studies by Vitek and Warlimont and by Ye. Z. Vintaykin and coworkers (16) have verified this prediction and Figure 13 shows that the metastable miscibility gap in the fcc phase of this system provides the basis for attaining high damping in Incramute and other Cu-Mn alloys via heat treatment.

The second phase of the study of damping in the 80 w/o Co-20 w/o Fe alloy currently under investigation is the evaluation of alloying additions on damping and strength. These activities were initiated during the past three months and have thus far demonstrated that substantial increases in strength can be obtained. However, the optimum "trade off composition" has not yet

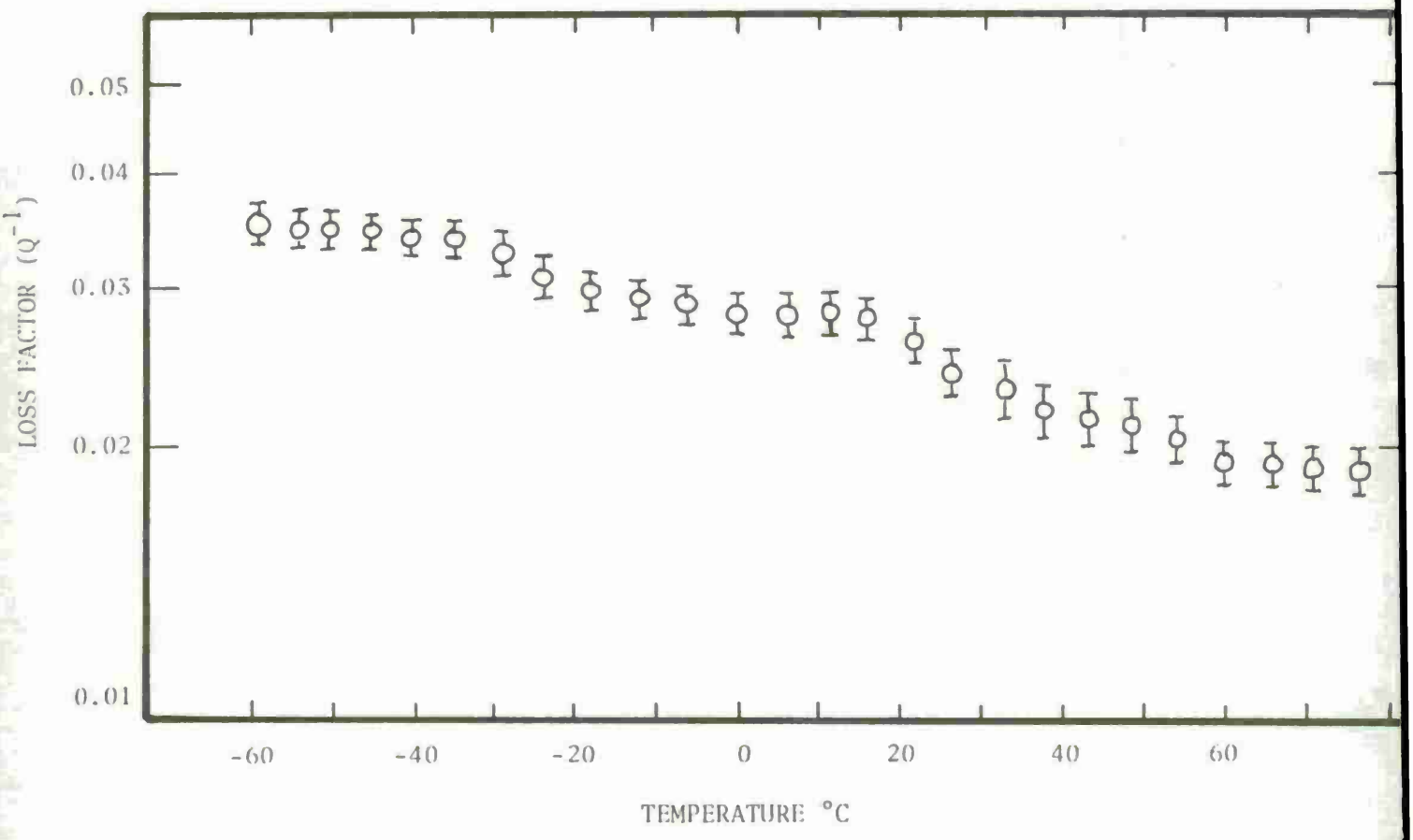

Figure 10. Loss Factor vs. Temperature Curve for a Sample of 80.5 w/o Co-19.5 w/o Fe measured at 240-250 Hertz and a stress of 2000 psi. The dynamical Young's Modulus measured over the same temperature range varied from 24 million psi at -60°C to 23 million psi at +80°C. The sample was annealed at 1000°C and air cooled.

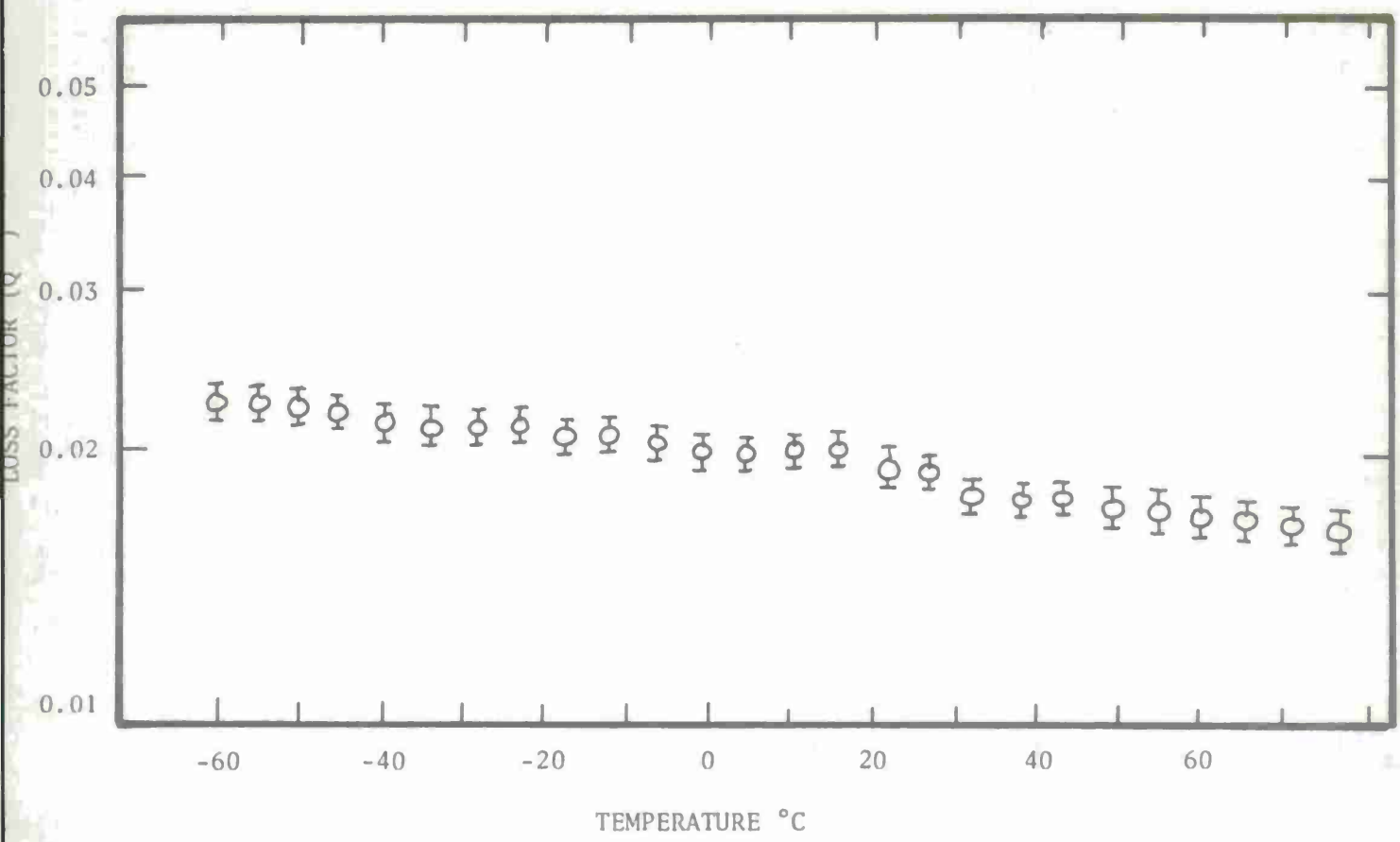

Figure 11. Loss Factor vs. Temperature Curve for a Sample of 81.5 w/o Co-18.5 w/o Fe measured at 240-250 Hertz and a stress of 2000 psi. The dynamical Young's Modulus measured over the same temperature range varied from 24 million psi at -60°C to 23 million psi at +80°C. The sample was annealed at 1000°C and air cooled.

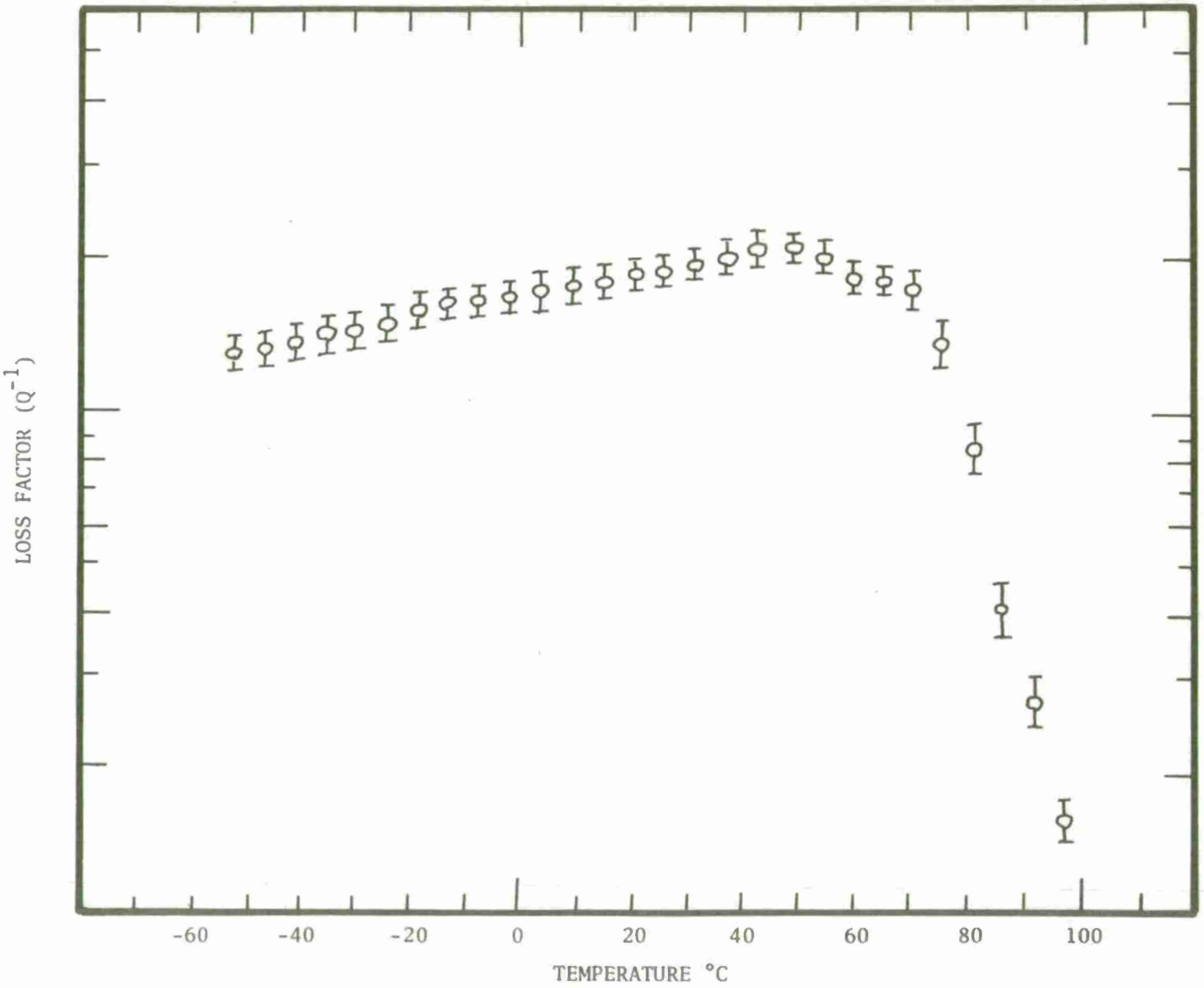

Figure 12. Loss Factor vs. Temperature for a Sample of Incramute I (Nominal Composition 55 w/o Cu-43 w/o Mn-2 w/o Al) heat treated for maximum damping characteristics and measured at 180-220 Hertz at a peak stress of 2000 psi. The dynamical Youngs Modulus varied from 12.5 Million psi at 100°C to 15.5 Million at -60°C.

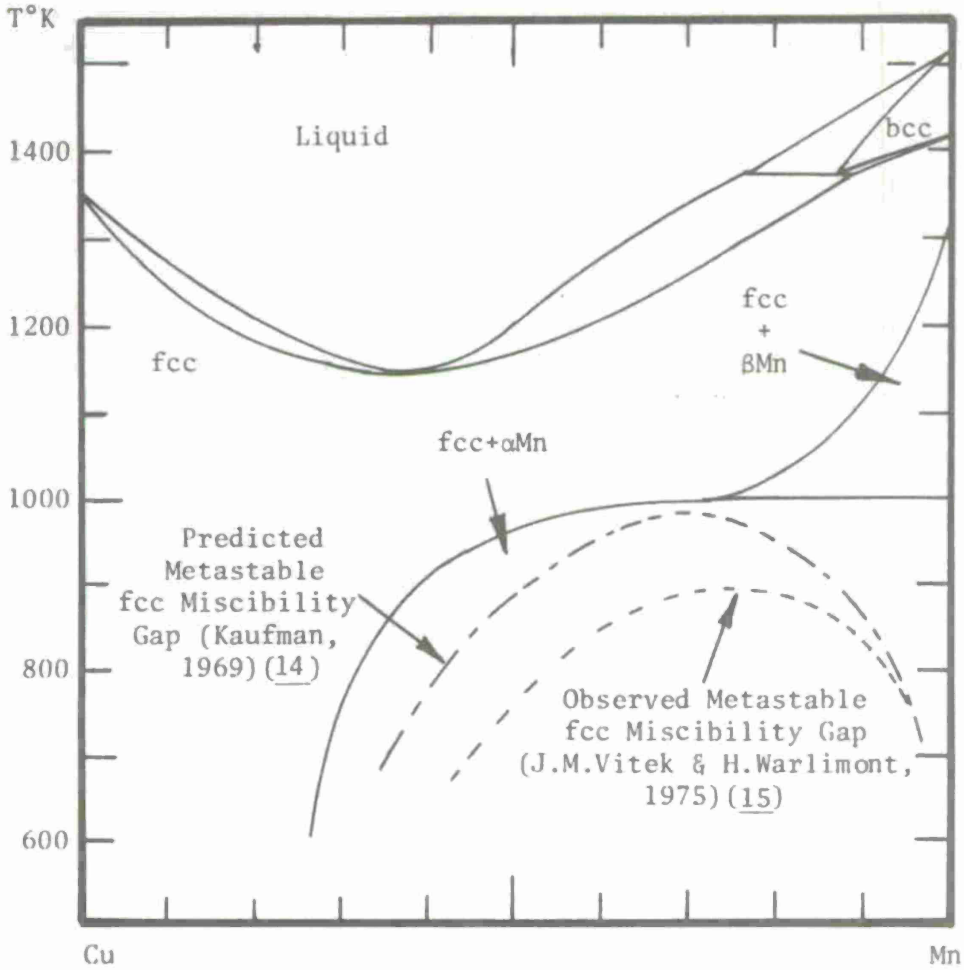

Figure 13. Predicted (14) and Observed (15) Metastable Miscibility Gaps in the Cu-Mn System.

been identified.

Table 3 shows the preliminary results which have been obtained. This compilation shows results of alloy synthesis, fabrication damping and tensile tests on eight alloys based on the Co-Fe composition with substantial additions of nickel or small additions of manganese or aluminum. These results were employed in constructing the bar graph shown in Figure 1.

The results obtained thus far indicate that the additions of nickel do not offer any substantial improvement in strength. However, very substantial increases in strength have been attained with aluminum and manganese. These improvements have been accompanied with a decrease in damping capacity. Nevertheless it is interesting to note that sample number 102 (76 w/o Co-19 w/o Fe-5 w/o Mn) exhibited twice the damping capacity of NIVCO at a comparable strength level (see Figure 1) while sample 99 (76 w/o Co-18 w/o Fe-6 w/o Al) exhibited a yield strength of 182,000 psi versus 110,000 psi for NIVCO at the same level of damping capacity which NIVCO exhibits (2). Thus the current results suggest that the alloying studies should be pursued.

TABLE 3

SUMMARY OF 0.2 PERCENT OFFSET YIELD STRENGTH AND
RESONANT DWELL DAMPING MEASUREMENTS AT 25° (Peak Stress 2000 PSI)
(ALL SAMPLES WERE MACHINED THEN ANNEALED
AT 1000°C AND AIR COOLED)

Sample No. Composition (weight percent)	Resonant Frequency (Hz.)	Dynamical Youngs Modulus (PSI x 10^{-6})	Loss Factor	0.2 Percent Offset Yield Strength (PSI)
85-(60Co-28Fe-12Ni)	243	24.0	0.0026	23100
86-(60Co-28Fe-12Ni)	246	24.6	0.0056	32400*
87-(50Co-32Fe-18Ni)	243	24.0	0.0026	30000
88-(40Co-38Fe-22Ni)	225	20.6	0.0016	29800
94-(72Co-18Fe-10Mn)	264	28.3	0.0011	53700
95-(72Co-18Fe-10Mn)	275	30.7	0.0008	87700*
97-(78Co-19Fe-3Al)	255	26.4	0.0015	25000
98-(78Co-19Fe-3Al)	240	23.4	0.0029	29900*
99-(76Co-18Fe-6Al)	273	30.3	0.0013	182000
100-(76Co-18Fe-6Al)	268	29.2	0.0011	157000*
101-(76Co-19Fe-5Mn)	262	27.9	0.0010	83800
102-(76Co-19Fe-5Mn)	264	28.3	0.0027	105700*
103-(77Co-19Fe-4Al)	271	30.1	0.0015	145000
104-(77Co-19Fe-4Al)	269	29.4	0.0011	152000*

*Cold Worked

III. INVESTIGATION OF COPPER-ALUMINUM-NICKEL ALLOYS FOR APPLICATION AS HIGH DAMPING STRUCTURAL MATERIALS

Since a damping member of significant size will most certainly have to be polycrystalline, it is essential to determine the effect of grain size on the transformation behavior. Accordingly, the various transformation characteristics (i.e. where the martensitic transformation begins and ends) of the Cu-14.01Al-3.0Ni alloy has been studied as a function of grain size. It is also important to determine the effects of grain size from a more fundamental aspect in order to establish the thermodynamics of this system (and a general model for other thermoelastic alloys).

It has been recognized by Tong and Wayman (17) that stored elastic strain energy (i.e. nonchemical free-energy contributions) can affect the A_s (the temperature of the start of reversion of the martensite back to the parent structure). In particular, they noted that A_s could lie below T_o. Such is not the case in nonthermoelastic systems. Tong and Wayman, however, considered that the contribution of the strain energy was negligible at M_s (the start temperature of the parent-to-martensite transformation) as well as at A_f (the finish temperature for the martensite-to-parent reversion). By assuming the elastic (nonchemical) free-energy contributions to be minimal in this range, Tong and Wayman placed T_o (i.e. the temperature where the total chemical energy of the parent equals that of the martensite) between M_s and A_f.

The contribution of strain energy to the transformation behavior has also been treated by Olson and Cohen (18). In this analysis, the strain energy is shown to be an important factor during the entire transformation and specifically, if a plate is formed in thermoelastic equilibrium. that this plate will revert at a temperature below T_o. Therefore, not only A_s but also A_f will be below T_o for the case of thermoelastic equilibrium. There are, however, two factors which can cause A_f to move above T_o in an otherwise thermoelastic alloy.

First, the interface between the martensite and the parent phase may have a frictional stress connected with its motion, and the finite stress required to move this interface can cause a deviation from thermoelastic behavior. Then, if the frictional stress is large enough, A_f may be displaced above T_o. Another deviation from thermoelasticity is evident when the strain energy associated with the transformation is not stored elastically in the system. If the strain energy is accommodated by plastic (nonrecoverable) slip, the system is nonthermoelastic -- most ferrous martensites are examples of this type. Moreover, the transformational shape change may not be elastically accommodated in certain other circumstances, the single-interface transformation in a single crystal being an important example. In the single-interface transformation, the macroscopic shape of the crystal is not constrained by grain boundaries (as it is in polycrystalline samples), and thus the transformational strain is not elastically stored; instead, the external shape of the crystal is changed. The amount of strain energy stored in the alloy may also be reduced in certain (usually large-grained) polycrystalline samples.

In order to experimentally determine some of the effects of grain size on the transformation characteristics, M_s, M_f, A_s, and A_f were measured on a number of samples of Cu-14.0Al-3.0Ni. These various transformation temperatures were observed optically by making use of the color change (copper-red to gold-yellow) that accompanies the parent-to-martensite transformation. Figure 14 shows the behavior of a single crystal Cu-14.0Al-3.0Ni sample which was cooled so as to transform it by a single-interface as well as by a multiple-interface sequence. The lowering of M_f and A_s in the multiple-interface transformation shows the contribution of the elastic energy. The A_f is very nearly the same in both cases because the final plate to transform (in the multiple-interface transformation) has no stored elastic energy to affect it.

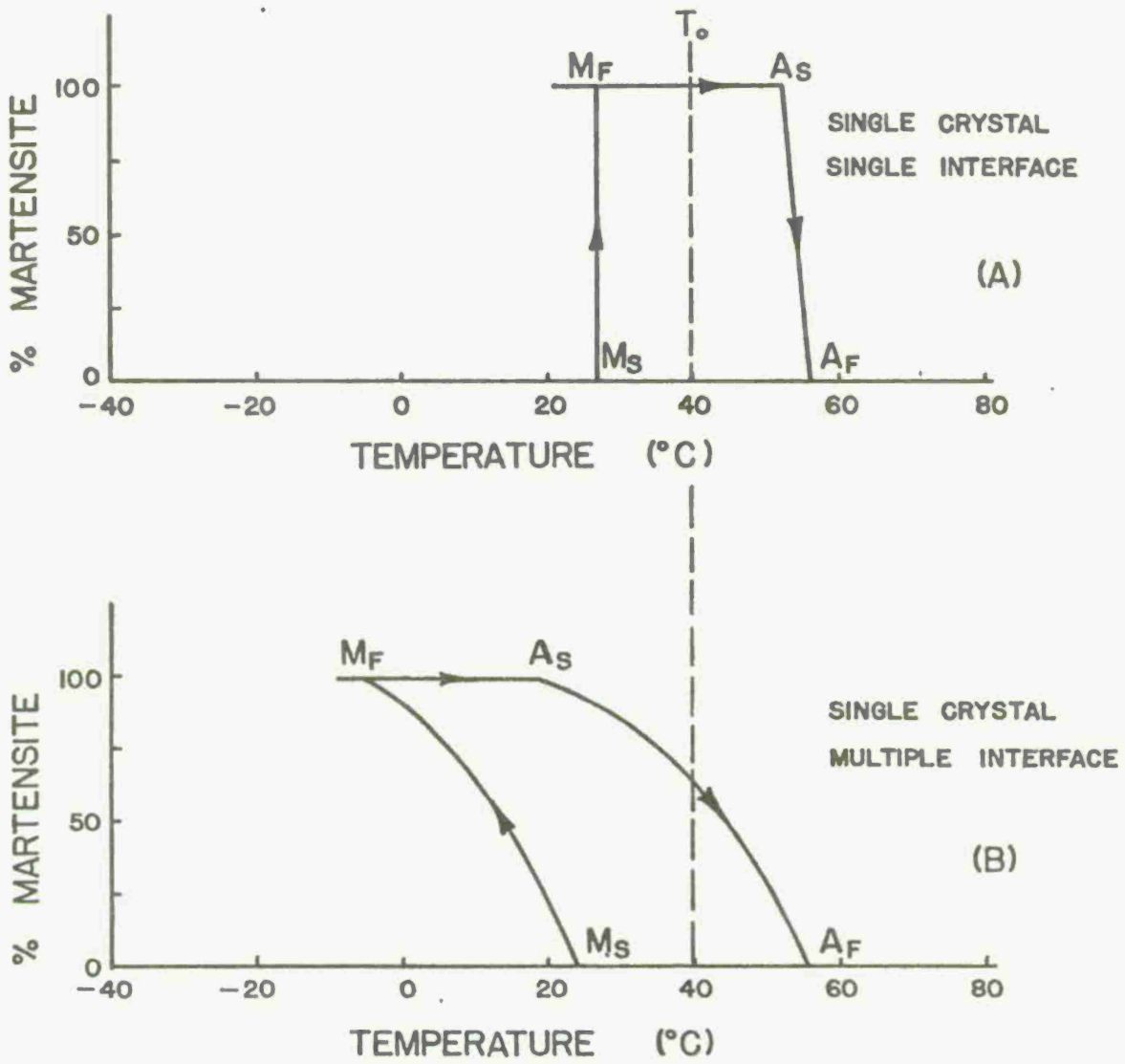

Figure 14. Transformation Hysteresis Curves for a Single Crystal Cu-14.0Al-3.0Ni for (A) Single Interface Transformation and (B) Multiple Interface Transformation.

Samples of Cu-14.0Al-3.0Ni alloy with differing grain size were viewed under a microscope while being cooled and heated in order to determine the transformation temperatures. The results are shown in Figure 15. The single crystal sample (Figure 15) was obtained by spark machining away the largest grain from the coarse-grained sample previously tested. Thus, the differences in the hysteresis loops between the coarse-grained sample and the single crystal sample are due entirely to constraints imposed by the grain boundaries and are not due to compositional changes. The hysteresis loop is shown in Figure 15 to be depressed with decreasing grain size. A_f is depressed in going from the single crystal to the polycrystal, but is not very strongly affected by the decreasing grain size of the samples tested.

Since the single crystal sample (nonsingle-interface transformation) has a negligible amount of stored elastic energy, both near M_s and A_f, then T_o can properly be bracketed by these temperatures. Taking $T_o = (A_f - M_s)/2$ (single crystal), T_o is about 31°C in this case. However, using $T_o = (A_f - M_s)/2$ in the polycrystalline case, as suggested by Tong and Wayman, leads to a T_o of 15-19°C. Since the hysteresis-loop width in this Cu-14.0Al-3.0Ni sample is on the order of 20 to 30°C, the difference in the T_o's obtained by these different methods is significant.

The effect of polycrystalline constraint is shown in Figure 16. In a single specimen within a small area, a variation in grain size could be seen. A small (about 0.02 in^2 in area) interior (i.e. away from edges and corners) was examined, and its M_s and A_f can be compared to those of a larger (about 0.04 in^2 in diameter) interior grain. These results can also be compared with less constrained grains (of about the same size) near the edges. Figure 16 shows that when the grain is less constrained, the M_s is raised significantly and, to a lesser extent, the A_f is also raised. The increase of the A_f (with decreasing amount of constraint) may be explained by the corresponding decrease in

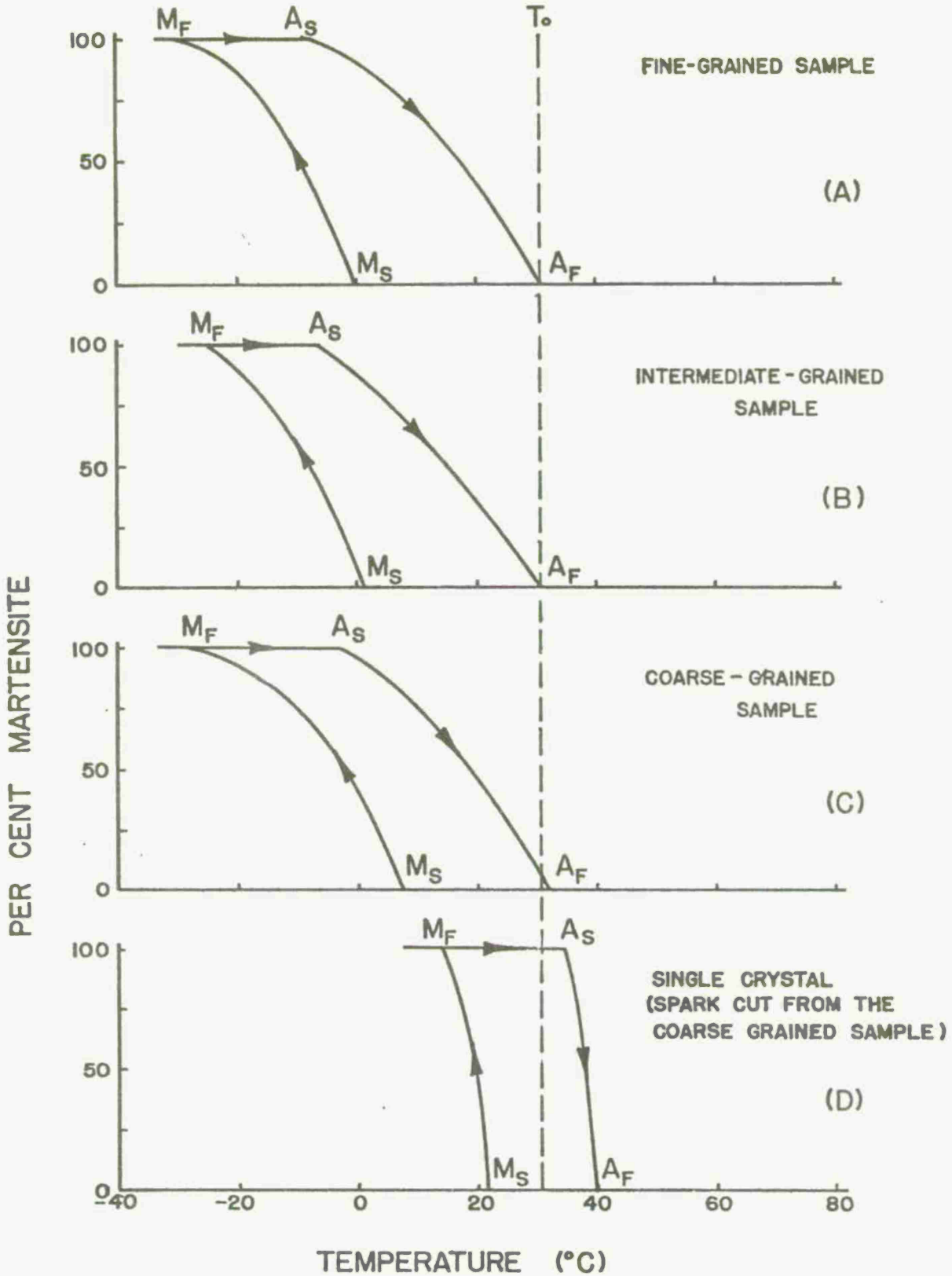

Figure 15. Transformation Hysteresis Curves for Cu-14.0Al-3.0Ni as a Function of Grain Size (A) Fine Grained (G.S.= 40 grains/in^2), (B) Intermediate Grained (G.S.= 60 grains/in^2), (C) Coarse Grained (G.S.=90 grains/in^2) and (D) Single Crystal (cut from the coarse-grained sample).

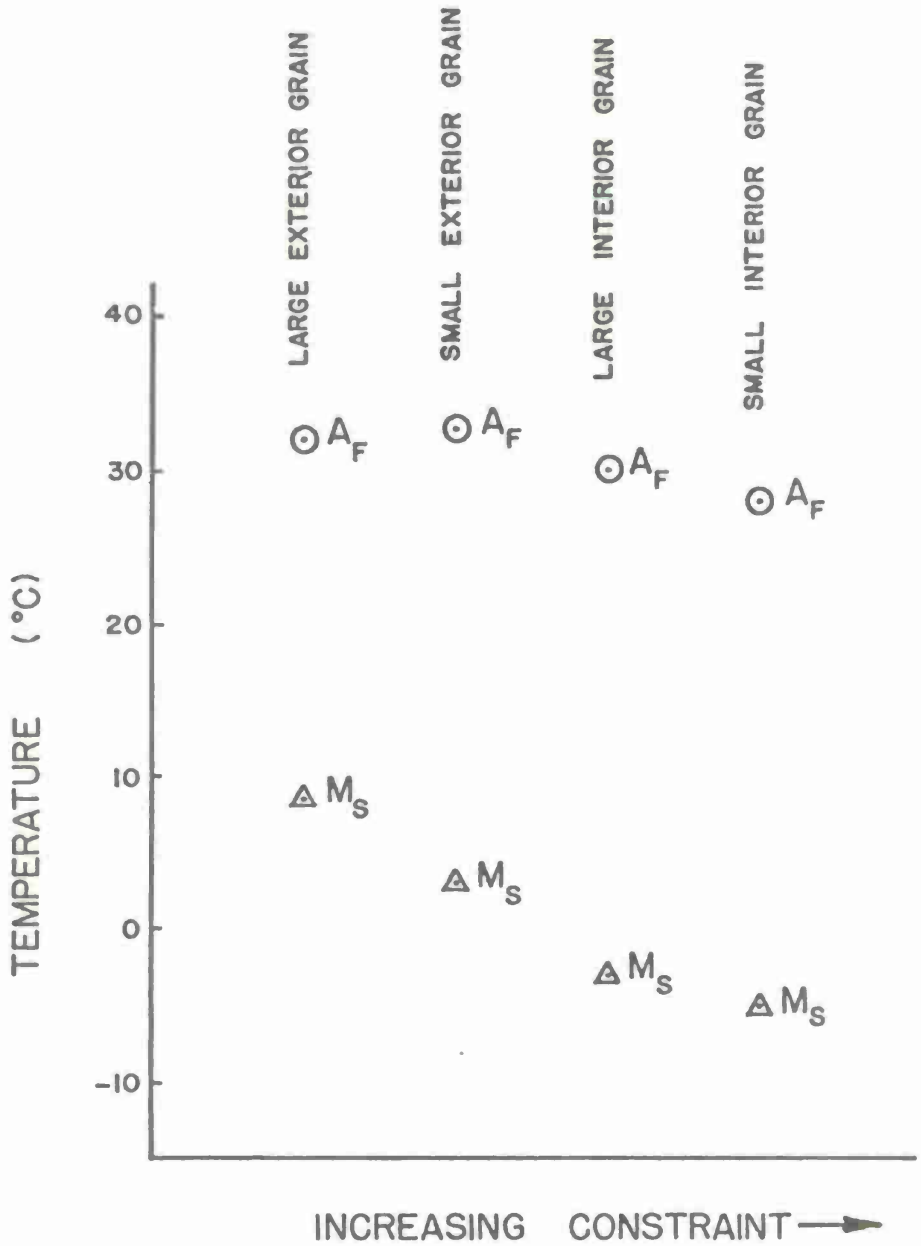

Figure 16. M_S and A_f Temperatures as a Function of Increasing Constraint on the Grain.

stored elastic energy. The even stronger effect on M_s cannot be entirely explained at the present time, but is undoubtedly associated with the effect of elastic constraints on the growth of the martensite. It is, however, surprising that the effect on M_s is so large, and further work is continuing on this problem.

Electrical resistivity has been measured as a function of temperature, and can be used as an alternate method of determining M_s, M_f, A_s and A_f. Figure 17 shows the resistivity versus temperature curve for a Cu-14.0Al-3.0Ni single crystal. The transformation temperatures cannot be compared quantitatively with the single crystal hysteresis loops in Figures 14 and 15 because even the minor differences in quenching rate from the solutionizing temperature of 950°C can change the degree of long-range order and this affects the transformation temperatures. However, it was noted that the temperatures where the color changes occurred coincided with the points of resistivity inversion, thus confirming the validity of determining the transformation temperatures on cooling and heating by the optical (color change) method.

The problem of brittleness in polycrystalline Cu_3Al-based alloys is of considerable importance in developing a useful alloy. The phase diagram of the Cu-Al system indicates that the equilibrium structure of Cu_3Al is the γ_2 phase, a brittle hcp structure. In the foundry industry, Cu-Al alloys with more than 10 w/o Al are avoided because of the extreme brittleness caused by the γ_2 phase. It has also been claimed (19) that the retained β_1 phase is instrumental in causing brittleness in Cu-Al alloys. When nickel is added to the Cu-Al alloys, further difficulties may be encountered because of brittle Ni-Al intermetallic compounds. In Cu-Al-Ni polycrystalline samples, the embrittlement is so severe that essentially no plastic deformation can be induced prior to intergranular fracture. By optical examination, the main problem seems to be the formation of a precipitate at the grain boundaries. Accordingly, a typical solution would be to increase the grain-boundary area and to break-up the continuity

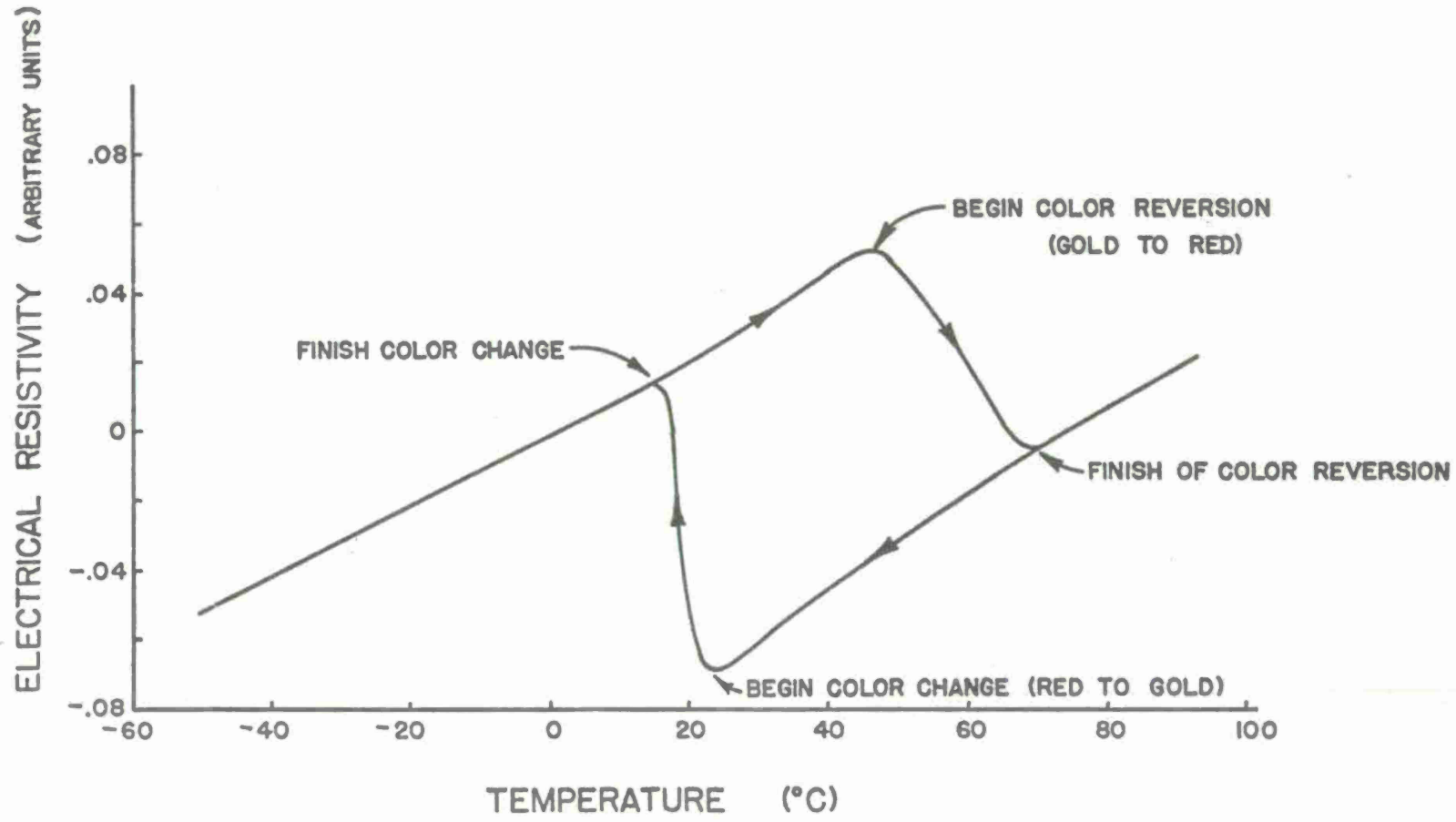

Figure 17. Transformation Hysteresis Curve for a Cu-14.0Al-3.0Ni Single Crystal Determined by Electrical-Resistance Measurement.

of the grain-boundary precipitate; this result is often accomplished in various alloy systems by hot working.

Samples of the Cu-Al-3.0Ni alloy containing from 12 to 14.2 w/o Al were hot rolled at temperatures from 550 to 900°C, the reduction usually being greater than 50% (after several passes). A small but noticeable increase in ductility in alloys of 12.6 w/o Al and 13.8 w/o Al was achieved by hot rolling at 800°C (80% in 5-10 passes) and water quenching directly from the rolls. The increase in ductility was, however, not large enough to be of practical interest. (A sample ~1/16 inch thick by about 3 inches long could only be bent to a radius of curvature of about 15 inches.) These thermomechanical treatments of the Cu-Al-Ni alloys had a negligible effect on the grain size (the average grain size stayed at about 30 grains/in^2) throughout the processing. The major effect of the hot rolling and quenching seemed to lie in the breaking-up of the precipitates at the grain boundaries (as seen in the optical microscope).

To refine the grain size of cast Cu-Al alloys in practice, the most common element added is Fe; Mn is also used in some cases. The additions of Fe and Mn are also known to depress the M_s in Cu-Al alloys (Ni was added to the Cu-Al alloys in order to depress the M_s from about 150-300°C to near room temperature). Thus, the additions of Fe and/or Mn to replace Ni in the Cu-Al alloys were hoped to have two beneficial effects. The first was that the Fe and Mn would refine the grain size and thereby present more grain-boundary area to any brittle precipitate--enough to make it noncontinuous at the grain boundaries. Secondly, the replacement of Ni by Fe and Mn might rid the system of any troublesome (very brittle) Ni-Al precipitates.

A series of samples of Cu-14.0Al with additions of 2 to 6 w/o Mn and 3 to 5 w/o Fe were induction-melted under a partial argon atmosphere and cast into an iron mold. The samples were solutionized at 950°C and quenched; those containing 4 to 6 w/o Mn

cracked on quenching. The as-quenched samples of 2 and 3 w/o Mn (at room temperature) showed an equiaxed structure (retained β_1) with clear evidence of precipitates at the grain boundaries. The 3 to 5 w/o Fe alloys were fully transformed to martensite at room temperature and also showed evidence of grain-boundary precipitation as well as fine precipitates dispersed throughout the matrix. Table 4 summarizes the effects of Mn and Fe additions on the grain size of the cast Cu-Al alloys. The Mn lowered the M_s to below room temperature (in the 3 w/o Mn alloy the M_s was below -20°C, and in the 6 w/o Mn alloy the M_s was below the liquid-nitrogen temperature). The Fe helped refine the grain size but seemed to have little effect in reducing M_s (heating the 5 w/o Fe sample to about 100°C caused no reversion).

The Cu-Al alloys containing Mn and Fe were hot rolled at 800°C; however, the hot rolling yielded no appreciable improvement in the ductility. The brittleness, therefore, seems to be little affected by the presence of Ni. There now remain two probable causes for the brittleness of the Cu-Al alloys. First the alloys of Cu-Al which contain greater than about 10 w/o Al have an equilibrium structure which is two phased ($\alpha + \gamma_2$) at room temperature, and it seems as though the formation of the brittle γ_2 phase at grain boundaries cannot be fully suppressed even with fairly fast quenching from the β_1 field (i.e. quenching into iced brine from 950°C).

Secondly, compression tests on the β_1 phase of Cu-14.1Al-3.0Ni single crystals by Shepard (International Symposium on Shape Memory Effects and Applications, Toronto, 1975, in press) indicate that normal slip is very difficult (at best) in this alloy. The single crystal samples of (100) orientation were stressed to 100 ksi with no indication of nonrecoverable plastic flow (i.e. plastic flow caused by slip yielding). The only exception was the development of kink bands in some single crystal orientations. These results suggest that, when stress-induced transformations

TABLE 4

EFFECT OF Mn AND Fe ADDITIONS

ON THE GRAIN SIZE OF Cu-14.0 w/o Al

Addition (w/o)	Grain Size (grains/in^2)
2% Mn	30-35
3% Mn	35-40
4% Mn	∿45
5% Mn	∿55
6% Mn	∿70
3% Fe	∿50
4% Fe	∿65
5% Fe	∿200

take place in polycrystalline Cu-Al-Ni alloys, the compatibility requirement that five independent deformation systems must operate in each individual grain can only be met by having at least five martensitic variants form within each grain. The stress (within the grain) needed to induce the formation of variants oriented nonpreferentially to the macroscopically-applied stress may be sufficiently high to cause fracture at the grain boundaries. The combination of the brittle intermetallics (at the grain boundaries) and the lack of dislocation-caused plasticity in this case seem to work together to make Cu-Al alloys lack any appreciable ductility. Solutions to this problem would seem to involve first the removal of the brittle precipitates at the grain boundary (thus making the grain boundary more glissile), and second to lower the dislocation flow stress. Lowering the dislocation flow stress would allow the proper stress compatibility conditions to operate at the grain boundaries.

REFERENCES

1. S. A. Kulin, L. Kaufman and P. P. Neshe, "Noise Abatement and Internal Vibrational Absorption in Potential Structural Materials," AMMRC CTR 74-53, Contract DAAG46-74-C-0048, ARPA Order 2555, December 1974, ManLabs, Inc., Cambridge, Massachusetts 02139.

2. L. Kaufman, S. A. Kulin and P. P. Neshe, "Noise Abatement and Internal Vibrational Absorption in Potential Structural Materials," AMMRC CTR 75-4, Contract DAAG46-74-C-0048, ARPA Order 2555, March 1975, ManLabs, Inc., Cambridge, Massachusetts 02139.

3. A. Cochardt, Tr. A.I.M.E. (1956) 206 1295.

4. A. Cochardt, Magnetic Properties of Metals and Alloys, A.S.M., Cleveland (1959) 251-279.

5. J. C. Fister and S. Shapiro, "Improved High Damping Copper-Base Alloys," International Copper Research Association Project 221, Final Report, September 1974, Olin Metals Research Laboratories, New Haven, Connecticut 06504.

6. J. Perkins, G. R. Edwards and N. Hills, "Materials Approaches to Ship Silencing," June 1974, NPS-59Ps74061, Naval Post Graduate School, Monterey, California.

7. J. F. Nachman, J. C. Napier and A. N. Hammer, "Development of Cu-Mn Base Alloys with High Damping Properties," International Copper Research Association Report No. 152, Final Report, March 1970, Solar Division, International Harvester Corporation, San Diego, California 92112.

8. J. F. Nachman, J. C. Napier and A. N. Hammer, "Development of Cu-Mn Base Alloys with High Damping Properties," International Copper Research Association Project No. 152A, Final Report, March 1971, Solar Division, International Harvester Corporation, San Diego, California 92112.

9. L. Kaufman and H. Nesor, Zeit. Metallkunde (1973) 74 249.

10. K. C. Mills, M. J. Richardson and P. J. Spencer, "Thermodynamic Properties and Phase Diagram of the Fe-Co and Ni-Pt Systems," Faraday Soc. Symposium (In Press).

11. H. Schumann, "Cobalt," (1968) 40 156.

12. U. Hashimoto, J. Japanese Inst. of Metals (1937) 1 177.

13. K. Ishida and T. Nishizawa, Tr. Jap. Inst. of Metals (1974) 15 225.

14. L. Kaufman, Metallurgical Transactions (1969) 245 91.

15. J. M. Vitek and H. Warlimont (1975)(Submitted for publication in Metal Science).

16. Ye. Z. Vintaykin, D. F. Litvin and V. A. Udorenko, Fiz. Metal. Metall., 37 no. 6, 1974, 1228.

17. H. Tong and C. M. Wayman, Acta Met. (1974) 22 887.

18. G. Olsen and M. Cohen (To be published in Acta Metallurgica).

19. B. Heyer, Engineering Physical Materials, Van Nostrand (1939).

TECHNICAL REPORT DISTRIBUTION

No. of Copies	To
1	Office of the Director, Defense Research and Engineering, The Pentagon, Washington, D. C. 20301
12	Commander, Defense Documentation Center, Cameron Station, Building 5, 5010 Duke Street, Alexandria, Virginia 22314
1	Metals and Ceramics Information Center, Battelle Memorial Institute, 505 King Avenue, Columbus, Ohio 43201
	Chief of Research and Development, Department of the Army, Washington, D. C. 20310
2	ATTN: Physical and Engineering Sciences Division
	Commander, Army Research Office (Durham), Box CM, Duke Station, Durham, North Carolina 27706
1	ATTN: Information Processing Office
	Commander, U. S. Army Materiel Command, 5001 Eisenhower Ave., Alexandria, Virginia 22304
1	ATTN: AMCRD-TC
	Commander, Deseret Test Center, Fort Douglas, Utah 84113
1	ATTN: Technical Information Office
	Commander, U. S. Army Electronics Command, Fort Monmouth, New Jersey 07703
1	ATTN: AMSEL-GG-DD
1	AMSEL-GG-DM
	Commander, U. S. Army Missile Command, Redstone Arsenal, Alabama 35809
1	ATTN: Technical Library
1	AMSMI-RSM, Mr. E. J. Wheelahan
	Commander, U. S. Army Armament Command, Rock Island, Illinois 61201
1	ATTN: AMSAR-SC, Dr. C. M. Hudson
1	AMSAR-PPW-PB, Mr. Francis X. Walter
2	Technical Library
	Commander, U. S. Army Satellite Communications Agency, Fort Monmouth, New Jersey 07703
1	ATTN: Technical Document Center
	Commander, U. S. Army Tank-Automotive Command, Warren, Michigan 48090
2	ATTN: AMSTA-BSL, Research Library Branch
	Commander, White Sands Missile Range, New Mexico 88002
1	ATTN: STEWS-WS-VT

No. of Copies	To
	Commander, Aberdeen Proving Ground, Maryland 21005
1	ATTN: STEAP-TL, Bldg. 305
	Commander, Frankford Arsenal, Philadelphia, Pennsylvania 19137
1	ATTN: Library, H1300, Bl. 51-2
	Commander, Picatinny Arsenal, Dover, New Jersey 07801
1	ATTN: SMUPA-RT-S
	Commander, Redstone Scientific Information Center, U. S. Army Missile Command, Redstone Arsenal, Alabama 35809
4	ATTN: AMSMI-RBLD, Document Section
	Commander, Watervliet Arsenal, Watervliet, New York 12189
1	ATTN: SWEWV-RDT, Technical Information Services Office
	Commander, U. S. Army Foreign Science and Technology Center, 220 7th Street, N. E., Charlottesville, Virginia 22901
1	ATTN: AMXST-SD3
	Director, Eustis Directorate, U. S. Army Air Mobility Research and Development Laboratory, Fort Eustis, Virginia 23604
1	ATTN: Mr. J. Robinson, SAVDL-EU-SS
	Librarian, U. S. Army Aviation School Library, Fort Rucker, Alabama 36360
1	ATTN: Building 5907
	Commander, USACDC Ordnance Agency, Aberdeen Proving Ground, Maryland 21005
2	ATTN: Library, Building 305
	Naval Research Laboratory, Washington, D. C. 20375
1	ATTN: Dr. J. M. Krafft - Code 8430
	Chief of Naval Research, Arlington, Virginia 22217
1	ATTN: Code 471
	Air Force Materials Laboratory, Wright-Patterson Air Force Base, Ohio 45433
2	ATTN: AFML (LAE), E. Morrissey
1	AFML (LC)
1	AFML (LMD), D. M. Forney
	National Aeronautics and Space Administration, Washington, D. C. 20546
1	ATTN: Mr. B. G. Achhammer
1	Mr. G. C. Deutsch - Code RR-1
	National Aeronautics and Space Administration, Marshall Space Flight Center, Huntsville, Alabama 35812
1	ATTN: R-P&VE-M, R. J. Schwinghamer
1	S&E-ME-MM, Mr. W. A. Wilson, Building 4720

No. of Copies	To
	Wyman-Gordon Company, Worcester, Massachusetts 01601
1	ATTN: Technical Library
	Defense Research Projects Agency, 1400 Wilson Boulevard, Arlington, Virginia 22209
5	ATTN: Dr. E. C. VanReuth
	National Science Foundation, 1800 G Street, Washington, D. C. 20550
1	ATTN: Dr Robert Reynik
1	Dr. Maurice Sinnott, University of Michigan, Assoc. Dir. of Engineering, Ann Arbor, Michigan 48104
	General Electric Company, Corporate Research and Development, Schenectady, New York 12301
5	ATTN: Mr. F. X. Gigliotti, Jr.
	Hitchiner Manufacturing Co., Inc., Elm Street, Milford, New Hampshire 03055
5	ATTN: Mr. G. D. Chandley
	Abex Corporation, Research Center, Mahwah, New Jersey 07430
5	ATTN: H. R. Larson
	Massachusetts Institute of Technology, Dept. of Metallurgy and Materials Science, Cambridge, Massachusetts 02139
5	ATTN: Dr. Merton C. Fleming
1	Fred E. Ziter, Adirondack Steel Casting Co., Shaker Road, Watervliet, New York 12189
1	Dr. Raymond J. Bratton, Westinghouse Electric Corporation Research Laboratory, Pittsburgh, Pennsylvania 15235
1	Lt. Col. Edward E. Chick, Chief, Materials Branch, U. S. Army R&D Group (Europe), Box 15, FPO New York 09510
1	TRW Equipment, TRW Inc., 23555 Euclid Avenue, Cleveland, Ohio 44117
1	ATTN: Elizabeth Barrett, T/M 3417
1	W. M. Spurgeon, Director, Mfg., Qual. Control & Home Systems, Program Management Center, Bendix Research Laboratories, Bendix Center Southfield, Michigan 48075
1	S. T. Wlodek, Director of Stellite R&D, Stellite Division, Cabot Corporation, 1020 West Park Avenue, Kokomo, Indiana 46901
	Deposite & Composites Inc., 1821 Michael Faraday Drive, Reston, Virginia 22090
1	ATTN: Richard E. Engdahl, President

No. of Copies	To
1	Mr. William A. Butler, Contract Administrator, Microwave Associates, Inc., Burlington, Massachusetts 01803
1	Mr. John A. Ulrich, Sr. Vice-President, Chamberlain Manufacturing Corp., Waterloo, Iowa 50705
1	A. V. Illyn, Technical Director, Babcock & Wilcox, Old Savannah Road, Augusta, Georgia 30903
1	Mr. W. J. Welsch (Code 224), Naval Materials Industry Resources Office, N.A.E.C., Building #537, Philadelphia, Pennsylvania 19112
1	Mr. R. E. Cross, Federal Die Casting Co., 2222 Elston Avenue, Chicago, Illinois 60614
1	Captain Ebenezer F. Porter, 2618 S. Lynn Street, Arlington, Virginia 22202
1	Mr. Charles E. Bates, Head, Metallurgy Section, Southern Research Institute, 2000 Ninth Avenue, South, Birmingham, Alabama 35205
	Director, Army Materials and Mechanics Research Center, Watertown, Massachusetts 02172
2	ATTN: AMXMR-PL
1	AMXMR-PR
1	AMXMR-CT
1	AMXMR-X
1	AMXMR-XC
1	AMXMR-ER
1	AMXMR-AP
1	Mr. R. F. Kirby, Chief, Materials Engineering Dept., Dept. 93-39M, Airesearch Manufacturing Company of Arizona, 402 South 36th Street, Phoenix, Arizona 85034

Army Materials and Mechanics Research Center
Watertown, Massachusetts 02172
NOISE ABATEMENT AND INTERNAL VIBRATIONAL ABSORPTION IN POTENTIAL STRUCTURAL MATERIALS
--L. Kaufman, S. A. Kulin, P. P. Neshe

Semi-Annual Report AMMRC CTR 76-3, January 1976
56 pp--illus-table, D/A Project ARPA 2555,
AMCMS Code 690000.21.10846

AD_____
UNCLASSIFIED
UNLIMITED DISTRIBUTION

Key Words
Titanium-nickel alloys
Vibration damping
Sound transmission
Internal friction
Iron-Cobalt Alloys
Copper-Aluminum-Nickel Alloys

Efforts have been directed toward achieving higher yield strengths in high damping cobalt-iron base alloys by adding nickel, aluminum and manganese. Substantial increases have been achieved through aluminum and manganese additions at low levels. The range of loss factors and yield strengths which are attainable exceed currently available commercial materials. Measurement of the temperature dependence of the loss factor of the cobalt-iron alloy for comparison with Nitinol and Incramute show that the cobalt-iron alloy retains a high loss factor up to 120°C while the latter materials exhibit a drop in loss factor well below 100°C. The effects of alloying additions of iron and manganese as well as reduction in grain size are being investigated as a means for reducing the brittleness of copper-aluminum-nickel alloys which exhibit thermoelastic martensitic transformations. These transformations provide high damping characteristics and high loss factors.

Army Materials and Mechanics Research Center
Watertown, Massachusetts 02172
NOISE ABATEMENT AND INTERNAL VIBRATIONAL ABSORPTION IN POTENTIAL STRUCTURAL MATERIALS
--L. Kaufman, S. A. Kulin, P. P. Neshe

Semi-Annual Report AMMRC CTR 76-3, January 1976
56 pp--illus-table, D/A Project ARPA 2555,
AMCMS Code 690000.21.10846

AD_____
UNCLASSIFIED
UNLIMITED DISTRIBUTION

Key Words
Titanium-nickel alloys
Vibration damping
Sound transmission
Internal friction
Iron-Cobalt Alloys
Copper-Aluminum-Nickel Alloys

Efforts have been directed toward achieving higher yield strengths in high damping cobalt-iron base alloys by adding nickel, aluminum and manganese. Substantial increases have been achieved through aluminum and manganese additions at low levels. The range of loss factors and yield strengths which are attainable exceed currently available commercial materials. Measurement of the temperature dependence of the loss factor of the cobalt-iron alloy for comparison with Nitinol and Incramute show that the cobalt-iron alloy retains a high loss factor up to 120°C while the latter materials exhibit a drop in loss factor well below 100°C. The effects of alloying additions of iron and manganese as well as reduction in grain size are being investigated as a means for reducing the brittleness of copper-aluminum-nickel alloys which exhibit thermoelastic martensitic transformations. These transformations provide high damping characteristics and high loss factors.